Resolving power and sensitivity to mismatch of optimum array processors

Henry Cox*

University of California, San Diego, Marine Physical Laboratory of the Scripps Institution of Oceanography, San Diego, California 92152

(Received 9 January 1973; revised 2 February 1973)

Mismatch in a beamformer occurs when the knowledge of the signal directional properties is imprecise. The effects of mismatch on a conventional beamformer and two optimum beamformers are compared. One optimum beamformer is based on inversion of the noise cross-spectral matrix while the other is based on inversion of the signal-plus-noise cross-spectral matrix. When there is mismatch, the inclusion of the signal in the matrix inversion process can lead to dramatic reductions in the output signal-to-noise ratio when the output signal-to-noise ratio of a perfectly matched beamformer would be greater than unity. However, the corresponding effect on the total beamformer output is less dramatic since an increase in the noise response partially offsets the decrease in signal response. The question of suppressing mismatched signals is closely related to the question of resolving closely spaced sources. Exact conditions are presented for resolution of closely spaced sources by an optimum beamformer. These results are applied to a line array and compared with the resolution capability of a conventional beamformer. It is found, for example, that an output signal-to-noise ratio of about 47 dB is required to achieve a resolving power with an optimum processor which is ten times that given by the classical Rayleigh limit. Conditions are also presented for the resolution of two sources of unequal strength.

Subject Classification: 15.3.

INTRODUCTION

Optimum array processors have received a great deal of attention in the last decade in a variety of application areas.[1–12] A fairly general array processing configuration is shown in Fig. 1. It consists of a beamformer which filters the output of each sensor and then sums the filtered outputs, followed by a single-channel postsummation processor. It is well known that the optimum processors under a variety of detection and estimation criteria can be structured to use the same beamformer and differ only in the postsummation processor. The optimum set of filters on the individual sensors depends on the inverse of the noise cross-spectral density matrix and the directional properties of the signal.

In many cases of practical importance it is not possible to obtain a signal-free estimate of the noise cross-spectral matrix. The measurable quantity is the cross-spectral matrix of the sensor outputs which in general contains signal plus noise. Indeed when there are multiple signal-like waves arriving from different directions even the definitions of signal and noise become somewhat arbitrary. While the use of the signal-plus-noise spectral matrix can also be optimum when the signal directional characteristics are known exactly, a problem of signal suppression arises when the knowledge of the signal directional characteristics is imperfect.

This paper is devoted to the analysis of two fundamental questions which arise in the use of the signal-plus-noise matrix in optimum beamforming. The first is the effect of "mismatch" which arises when there is imperfect knowledge about the signal directional characteristics. The second is the question of resolution, that of determining conditions under which the processor will indicate that the array is responding to waves from two spatially separated sources rather than to a wave from a single source.

In spite of the importance of these questions, they have largely been ignored in the literature and few quantitative results have been reported. Capon[13] coins the phrase "high resolution frequency-wavenumber estimation" for a procedure based on inversion of the signal-plus-noise matrix. He concludes that resolution greater than that of a conventional beamformer is attainable when the output signal-to-noise ratio is sufficiently high but provides no quantitative indication of how much signal-to-noise ratio is sufficient for resolution. Seligson[14] in commentating on Capon's paper concludes that the "high resolution estimator" may display less angular resolution than the conventional beamformer under conditions of mismatch. Actually, he examines the relative sharpness in the peaks of the bearing response patterns of the two

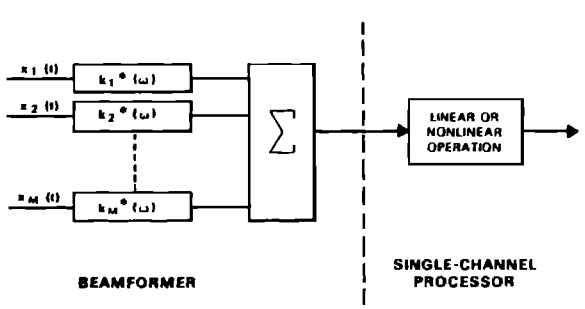

FIG. 1. Array processor configuration.

processors for the case of a single source. McDonough,[15] using a statistical analysis, concludes that Capon's processor may exhibit anomalous behavior when there are small random errors in the signal model if a certain measure of sensitivity is high. Cox[16] presents a general sensitivity analysis for beamformers of the type shown in Fig. 1, including some initial results on the question of mismatch.

In this paper the sensitivity to mismatch of the conventional beamformer, the beamformer based on the inverse of the noise cross-spectral matrix, and the beamformer based on inversion of the signal-plus-noise matrix are compared. The analysis of mismatched performance provides the basis for examining the more difficult problem of determining exact conditions under which two spatially separated sources will be resolved by an optimum beamformer based on inversion of the signal-plus-noise cross-spectral matrix. Resolving power of this optimum beamformer is compared with that of a conventional beamformer.

The approach in the paper emphasizes geometric aspects of these problems. The geometric approach leads to significant simplification of many of the basic results so that they are more easily understood. It also permits us to obtain new results with relative ease, in cases in which other approaches are discouragingly complicated.

I. BACKGROUND

Consider an array consisting of M omnidirectional sensors in an arbitrary known spatial configuration. The output of the ith sensor is a time series denoted by $x_i(t)$. The cross-correlation matrix of the M sensor outputs is defined to be the matrix with the following entry in its ith row and jth column:

$$r_{ij}(\tau)=\overline{x_i(t)x_j(t-\tau)}, \tag{1}$$

where the overbar denotes ensemble average. The cross-spectral matrix $\mathbf{R}(\omega)$ is the matrix which has as its i,jth entry the Fourier transform of the corresponding entry of the cross-correlation matrix. That is,

$$R_{ij}(\omega)=\int r_{ij}(\tau)\exp(-i\omega\tau)d\tau. \tag{2}$$

$\mathbf{R}(\omega)$ may be thought of as being composed of a number of components with differing spatial properties.

The components of particular interest to us correspond to waves emanating from point sources and propagating across the array. Such a coherent wave would contribute a component to $\mathbf{R}(\omega)$ of the following form:

$$\sigma_d^2(\omega)\mathbf{d}(\omega)\mathbf{d}^*(\omega),$$

where $\mathbf{d}(\omega)$ is a column matrix or vector, called the "direction vector" of the wave. The jth component of $\mathbf{d}(\omega)$ is the relative amplitude and phase of the component at the jth sensor. The notational convention used in this paper is that column matrices or vectors are represented by boldface lower-case letters. The asterisk denotes conjugate transposition. Boldface upper-case letters are used to denote Hermitian matrices. Thus $\mathbf{d}^*(\omega)$ is a row vector and $\mathbf{d}(\omega)\mathbf{d}^*(\omega)$ is a rank-one Hermitian matrix. The inner product $\mathbf{d}^*(\omega)\mathbf{d}(\omega)$ is normalized to be equal to M so that $\sigma_d^2(\omega)$ is the average input power spectrum of the wave, the average being made across the M sensors. For a plane wave received at all the sensors with equal intensity, $\mathbf{d}(\omega)$ would have the following form:

$$\mathbf{d}(\omega)=\begin{bmatrix}\exp\{i(\mathbf{p}_1\cdot\mathbf{u}_d)\omega/c\}\\ \exp\{i(\mathbf{p}_2\cdot\mathbf{u}_d)\omega/c\}\\ \vdots\\ \exp\{i(\mathbf{p}_M\cdot\mathbf{u}_d)\omega/c\}\end{bmatrix},$$

where $\mathbf{p}_j$ is the three-dimensional vector of position coordinates of the jth sensor, $\mathbf{u}_d$ is a unit vector in the direction from which the wave is propagating, and c is the velocity of propagation.

In most of the subsequent analysis it is not necessary to assume that the waves of interest are planar. The general results are equally applicable, for example, to nearfield focusing of arrays for imaging.

In the special case of plane waves, a fairly mild form of array symmetry leads to certain simplifications. An array will be called pairwise symmetric if for each sensor located away from the origin at position coordinates $\{x_j,y_j,z_j\}$ there is also a sensor located at $\{-x_j,-y_j,-z_j\}$. This type of symmetry is also known as inversion symmetry. Pairwise symmetric arrays have the property that if $\mathbf{d}(\omega)$ and $\mathbf{b}(\omega)$ are direction vectors corresponding to plane waves, then the inner product $\mathbf{d}^*(\omega)\mathbf{b}(\omega)$ is real.

The power spectrum of the output of the beamformer shown in Fig. 1 is given by the following Hermitian form:

$$z(\omega)=\mathbf{k}^*(\omega)\mathbf{R}(\omega)\mathbf{k}(\omega), \tag{3}$$

where $\mathbf{k}^*(\omega)$ is the row vector $\{k_1^*(\omega),\cdots,k_M^*(\omega)\}$ of the filter transfer function for each sensor.

Suppose that $\mathbf{R}(\omega)$ consists of signal-plus-noise so that we may express $\mathbf{R}(\omega)$ as the following sum:

$$\mathbf{R}(\omega)=\sigma_0^2(\omega)\mathbf{Q}(\omega)+\sigma_1^2\mathbf{d}(\omega)\mathbf{d}^*(\omega), \tag{4}$$

where $\sigma_0^2(\omega)\mathbf{Q}(\omega)$ is the noise component and $\mathbf{Q}(\omega)$ is normalized to have its trace equal to the number of sensors M. Then $\sigma_0^2(\omega)$ is the input noise spectral level averaged across the sensors. Recalling that $\mathbf{d}(\omega)$ is also normalized so that $\mathbf{d}^*(\omega)\mathbf{d}(\omega)=M$, it follows that $\sigma_1^2(\omega)/\sigma_0^2(\omega)$ is the input signal-to-noise spectral ratio. Substituting from Eq. 4 into Eq. 3 yields

$$z(\omega)=\sigma_0^2(\omega)\mathbf{k}^*(\omega)\mathbf{Q}(\omega)\mathbf{k}(\omega)+\sigma_1^2(\omega)\,|\mathbf{k}^*(\omega)\mathbf{d}(\omega)|^2. \tag{5}$$

Henceforth, we shall confine our attention to a single frequency and the dependence of various quantities on ω will not be shown explicitly. Many of the results

expressed in general vector–matrix form may be reinterpreted and applied directly to related problems.[10] The ratio of the two terms in Eq. 5,

$$(S/N)_0=\sigma_1^2|\mathbf{k}^*\mathbf{d}|^2/\sigma_0^2\mathbf{k}^*\mathbf{Q}\mathbf{k}, \quad (6)$$

is the output signal-to-noise spectral ratio and the quantity

$$G=|\mathbf{k}^*\mathbf{d}|^2/(\mathbf{k}^*\mathbf{Q}\mathbf{k}) \quad (7)$$

is the array gain or improvement in signal-to-noise ratio due to beamforming. We shall frequently write $G(\mathbf{k})$ and $z(\mathbf{k})$ to denote the array gain and output spectrum for a particular choice of the filter vector $\mathbf{k}$. From Eqs. 6 and 7 it is evident that $(S/N)_0$ and G do not change if $\mathbf{k}$ is multiplied by a scalar.

In many cases of practical importance the available information about the signal direction vector $\mathbf{d}$ is imprecise. This leads to the definition of the steering vector $\mathbf{m}$ as the vector which represents the assumed signal characteristics. The filter vector $\mathbf{k}$ is always a function of the steering vector $\mathbf{m}$. When $\mathbf{m}=\mathbf{d}$ the processor is said to be perfectly matched to the signal directional characteristics. Mismatch occurs when $\mathbf{m}\neq\mathbf{d}$. The steering vector $\mathbf{m}$ is also normalized so that $\mathbf{m}^*\mathbf{m}=M$. Some possible causes of mismatch are distortion in the wavefront during propagation, amplitude, phase and position errors in the sensors, sampling and quantization. In addition to these sources of mismatch, $\mathbf{m}$ will usually be scanned over some set of steering vectors which correspond to a class of interesting signals. For example, this set might correspond to plane waves from some angular region of interest or to spherical waves emanating from a spatial region near the array. Scanning away from the signal direction increases mismatch. This usually has the effect of producing a peak in the scanned array response at the steering vector $\mathbf{m}$ which corresponds most closely to the actual signal direction vector $\mathbf{d}$.

Three particular choices of the filter vector $\mathbf{k}$ will be examined in this paper. These are

$$\mathbf{k}_1=\mathbf{m}/M, \quad (8)$$

$$\mathbf{k}_2=\mathbf{Q}^{-1}\mathbf{m}/(\mathbf{m}^*\mathbf{Q}^{-1}\mathbf{m}), \quad (9)$$

and

$$\mathbf{k}_3=\mathbf{R}^{-1}\mathbf{m}/(\mathbf{m}^*\mathbf{R}^{-1}\mathbf{m}). \quad (10)$$

The denominators of Eqs. 8, 9, and 10 provide an additional normalization so that $\mathbf{k}^*\mathbf{m}=1$. Thus, the three processors all have a unit response to a unit signal from the assumed signal direction so they provide unbiased estimates of signals from that direction.

The first choice, $\mathbf{k}_1=\mathbf{m}/M$, is the conventional beamformer, which simply matches to the assumed signal directional characteristics.

The second choice, $\mathbf{k}_2=\mathbf{Q}^{-1}\mathbf{m}/(\mathbf{m}^*\mathbf{Q}^{-1}\mathbf{m})$, when perfectly matched and followed by an appropriate single-channel processor is optimum for a variety of detection and estimation problems. It reduces to the conventional processor when the noise is uncorrelated from sensor to sensor so that $\mathbf{Q}=\mathbf{I}$, the identity matrix. When perfectly matched, the gain of this processor is seen from Eq. 7 to be

$$G(\mathbf{k}_2)=\mathbf{d}^*\mathbf{Q}^{-1}\mathbf{d}, \quad \text{for } \mathbf{m}=\mathbf{d}. \quad (11)$$

The output signal-to-noise ratio is also maximized by the choice $\mathbf{k}=\mathbf{k}_2$. This maximum signal-to-noise is an important parameter in our analysis. Substituting from Eq. 9 into 6 yields

$$(S/N)_{max}=\mathbf{d}^*\mathbf{Q}^{-1}\mathbf{d}\sigma_1^2/\sigma_0^2. \quad (12)$$

The third choice, $\mathbf{k}_3=\mathbf{R}^{-1}\mathbf{m}/(\mathbf{m}^*\mathbf{R}^{-1}\mathbf{m})$, produces the same output spectrum as $\mathbf{k}_2$ does when both are perfectly matched. Hence, when perfectly matched, $\mathbf{k}_2$ and $\mathbf{k}_3$ produce the same gain and the same output signal-to-noise ratio. However, when there is mismatch these processors differ in interesting and important ways which we shall examine in some detail. The output spectrum for $\mathbf{k}_3$ may be found by substituting from Eq. 10 into Eq. 3 as follows:

$$z(\mathbf{k}_3)=\left(\frac{\mathbf{m}^*\mathbf{R}^{-1}}{\mathbf{m}^*\mathbf{R}^{-1}\mathbf{m}}\right)\mathbf{R}\left(\frac{\mathbf{R}^{-1}\mathbf{m}}{\mathbf{m}^*\mathbf{R}^{-1}\mathbf{m}}\right)=(\mathbf{m}^*\mathbf{R}^{-1}\mathbf{m})^{-1}. \quad (13)$$

With the advent of high-speed digital circuitry and FFT algorithms, it may be desirable to make direct computations on the sensor outputs rather than building a configuration resembling Figure 1. A procedure suggested by Eq. 13 is to obtain an estimate of $\mathbf{R}$ denoted by $\hat{\mathbf{R}}$ using a finite-length data sample and to compute

$$(\mathbf{m}^*\hat{\mathbf{R}}^{-1}\mathbf{m})^{-1}$$

for the set of steering vectors $\mathbf{m}$ of interest. This procedure has been called a "high resolution" estimator by Capon,[13] who suggests its use in seismic applications. Some results concerning bias and variance of this estimator have been given by Capon and Goodman.[17] In the limit as $\hat{\mathbf{R}}\rightarrow\mathbf{R}$ this procedure is equivalent to computing the output spectrum of a beamformer with $\mathbf{k}=\mathbf{k}_3$. Thus the analysis of this paper will provide asymptotic properties of this estimation procedure.

II. MATHEMATICAL PRELIMINARIES

This section presents some mathematical concepts and results which will be used repeatedly. The approach will be to emphasize geometric aspects of various relationships in an attempt to provide simple interpretations of what initially appear to be quite complicated expressions.

A. Sines and Cosines

A useful concept is that of a generalized angle between two vectors. Let $\mathbf{a}$ and $\mathbf{b}$ be M-component complex column vectors and let $\mathbf{C}$ be a positive definite Hermitian matrix. Then we may define an inner

product between $\mathbf{a}$ and $\mathbf{b}$ by $\mathbf{a}^*\mathbf{C}\mathbf{b}$ and let $H(\mathbf{C})$ denote the space of M-dimensional complex vectors with the inner product so defined. In this space it is natural to define the cosine-squared of the generalized angle between $\mathbf{a}$ and $\mathbf{b}$ as follows:

$$\cos^2(\mathbf{a},\mathbf{b};\mathbf{C})=|\mathbf{a}^*\mathbf{C}\mathbf{b}|^2/\{(\mathbf{a}^*\mathbf{C}\mathbf{a})(\mathbf{b}^*\mathbf{C}\mathbf{b})\}. \quad (14)$$

By the Schwarz inequality,

$$0\leq\cos^2(\mathbf{a},\mathbf{b};\mathbf{C})\leq 1. \quad (15)$$

The length of a vector $\mathbf{b}$ in $H(\mathbf{C})$ is $(\mathbf{b}^*\mathbf{C}\mathbf{b})^{\frac{1}{2}}$. When $\cos^2(\mathbf{a},\mathbf{b};\mathbf{C})=0$, the vectors $\mathbf{a}$ and $\mathbf{b}$ are orthogonal in $H(\mathbf{C})$. When $\cos^2(\mathbf{a},\mathbf{b};\mathbf{C})=1$, $\mathbf{a}$, and $\mathbf{b}$ are in perfect alignment in the sense that one is a scalar multiple of the other. It is natural to define $\sin^2(\mathbf{a},\mathbf{b};\mathbf{C})$ through the identity

$$\sin^2(\cdot)=1-\cos^2(\cdot). \quad (16)$$

Among the cases of interest in this paper are $\mathbf{C}=\mathbf{I}$, the identity matrix, and $\mathbf{C}=\mathbf{Q}^{-1}$, the inverse of the normalized noise cross-spectral matrix. When $\mathbf{C}=\mathbf{I}$ we will write $\cos^2(\mathbf{a},\mathbf{b})$ instead of $\cos^2(\mathbf{a},\mathbf{b};\mathbf{I})$ since no confusion will result.

In order to follow the developments of this paper it is sufficient to know the definitions of $\cos^2(\mathbf{a},\mathbf{b};\mathbf{C})$ and $\sin^2(\mathbf{a},\mathbf{b};\mathbf{C})$ given above. However, since the approach has broad applicability a few words of further explanation may be useful.

In order to better understand the effect of the metric $\mathbf{Q}^{-1}$ it is worthwhile to compare $\cos^2(\mathbf{a},\mathbf{b})$ and $\cos^2(\mathbf{a},\mathbf{b};\mathbf{Q}^{-1})$. To do this, consider the eigenvalues and corresponding orthonormal eigenvectors of $\mathbf{Q}$, which we denote by $\{\lambda_1,\cdots,\lambda_M\}$ and $\{\mathbf{e}_1,\cdots\mathbf{e}_M\}$, respectively. Since $\mathbf{Q}$ is normalized to have its trace equal to M, $\sum\lambda_i=M$. Representing $\mathbf{a}$ and $\mathbf{b}$ in terms of their projections on the eigenvectors of $\mathbf{Q}$ as follows:

$$\mathbf{a}=\sum_{i=1}^{M}h_i\mathbf{e}_i \quad \mathbf{b}=\sum_{i=1}^{M}g_i\mathbf{e}_i,$$

where

$$h_i=\mathbf{e}_i^*\mathbf{a} \quad g_i=\mathbf{e}_i^*\mathbf{b};$$

then

$$\cos^2(\mathbf{a},\mathbf{b})=|\sum h_i^*g_i|^2/(\sum|h_i|^2)(\sum|g_i|^2) \quad (17)$$

and

$$\cos^2(\mathbf{a},\mathbf{b};\mathbf{Q}^{-1})=\frac{|\sum h_i^*g_i/\lambda_i|^2}{(\sum|h_i|^2/\lambda_i)(\sum|g_i|^2/\lambda_i)}. \quad (18)$$

From Eqs. 17 and 18 it is apparent that the effect of the metric $\mathbf{Q}^{-1}$ is equivalent to scaling h_i and g_i by $(1/\lambda_i)^{\frac{1}{2}}$. This scaling emphasizes components of $\mathbf{a}$ and $\mathbf{b}$ corresponding to small eigenvalues of $\mathbf{Q}$, and de-emphasizes components corresponding to large eigenvalues of $\mathbf{Q}$. Since the small eigenvalues of $\mathbf{Q}$ correspond to components with less noise, it is natural that the metric $\mathbf{Q}^{-1}$ arises in optimization considerations.

The space $H(\mathbf{Q}^{-1})$ arises naturally when optimum processors are considered. It is closely related to the reproducing kernel Hilbert space approach which has been pioneered by Parzen[18] and emphasized by Kailath[19] in treating continuous parameter detection and estimation problems. Hence, by a suitable reinterpretation, many of the results of this paper can be extended to a more general abstract case.

B. Some Useful Relationships

In this section some relationships are presented which apply when $\mathbf{R}$ is of the following form:

$$\mathbf{R}=\sigma_0^2\mathbf{Q}+\sigma_1^2\mathbf{d}\mathbf{d}^*. \quad (19)$$

When $\mathbf{R}$ is given by Eq. 19, its inverse may be obtained using the following matrix identity:

$$\mathbf{R}^{-1}=(1/\sigma_0^2)\{\mathbf{Q}^{-1}-\mathbf{Q}^{-1}\mathbf{d}\mathbf{d}^*\mathbf{Q}^{-1}(\sigma_1^2/\sigma_0^2)\times(1+\mathbf{d}^*\mathbf{Q}^{-1}\mathbf{d}\sigma_1^2/\sigma_0^2)^{-1}\}. \quad (20)$$

Using the definition of $(S/N)_{max}$ given in Eq. 12, the following relationships follow directly from Eqs. 20, 14, and 16 as shown in Appendix A:

$$\mathbf{m}^*\mathbf{R}^{-1}\mathbf{m}=\frac{\mathbf{m}^*\mathbf{Q}^{-1}\mathbf{m}}{\sigma_0^2}\times\left\{\frac{1+(S/N)_{max}\sin^2(\mathbf{m},\mathbf{d};\mathbf{Q}^{-1})}{1+(S/N)_{max}}\right\}, \quad (21)$$

$$|\mathbf{m}^*\mathbf{R}^{-1}\mathbf{d}|^2=\frac{(\mathbf{m}^*\mathbf{Q}^{-1}\mathbf{m})(\mathbf{d}^*\mathbf{Q}^{-1}\mathbf{d})\cos^2(\mathbf{m},\mathbf{d};\mathbf{Q}^{-1})}{\sigma_0^4[1+(S/N)_{max}]^2}, \quad (22)$$

$$\mathbf{m}^*\mathbf{R}^{-1}\mathbf{Q}\mathbf{R}^{-1}\mathbf{m}=\frac{\mathbf{m}^*\mathbf{Q}^{-1}\mathbf{m}}{\sigma_0^4}\times\left\{\frac{1+[2(S/N)_{max}+(S/N)_{max}^2]\sin^2(\mathbf{m},\mathbf{d};\mathbf{Q}^{-1})}{[1+(S/N)_{max}]^2}\right\}. \quad (23)$$

III. MISMATCH

In this section expressions are obtained for the array gain and output spectrum of beamformers with filter vectors given by Eqs. 8, 9, and 10 under the assumption that $\mathbf{R}$ is given by Eq. 19.

A. Conventional Beamforming ($\mathbf{k}_1=\mathbf{m}/M$)

Substituting from Eq. 8 into Eq. 7 yields the following expression for gain of a conventional beamformer:

$$G(\mathbf{k}_1)=|\mathbf{m}^*\mathbf{d}|^2/(\mathbf{m}^*\mathbf{Q}\mathbf{m})=M^2\cos^2(\mathbf{m},\mathbf{d})/(\mathbf{m}^*\mathbf{Q}\mathbf{m}). \quad (24)$$

For spatially uncorrelated noise ($\mathbf{Q}=\mathbf{I}$), Eq. 24 reduces to

$$G(\mathbf{k}_1)=M\cos^2(\mathbf{m},\mathbf{d}). \quad (25)$$

Similarly, substituting from Eq. 8 into Eq. 5 results in the following expression for the output spectrum of a conventional beamformer:

$$z(\mathbf{k}_1)=\sigma_1^2\cos^2(\mathbf{m},\mathbf{d})+\sigma_0^2(\mathbf{m}^*\mathbf{Q}\mathbf{m})/M^2. \quad (26)$$

The first term in Eq. 26 is due to the signal and the second term is due to the noise. From Eq. 26 it is evident that the quantity $\cos^2(\mathbf{m},\mathbf{d})$ is simply the power response of a conventional beamformer steered in "direction" $\mathbf{m}$ to a unit signal from "direction" $\mathbf{d}$. Plotting $\cos^2(\mathbf{m},\mathbf{d})$ when the signal direction vector $\mathbf{d}$ is varied over the set of plane waves for a fixed steering direction vector $\mathbf{m}$ results in the familiar beam pattern.

Notice that the signal response of a conventional beamformer depends on the cosine squared of the generalized angle between $\mathbf{m}$ and $\mathbf{d}$ in $H(\mathbf{I})$, and is not influenced by the noise matrix $\mathbf{Q}$. Moreover, mismatch does not affect the noise component directly but only through the factor $(\mathbf{m}^*\mathbf{Q}\mathbf{m})$ appearing in Eq. 26 instead of the factor $(\mathbf{d}^*\mathbf{Q}\mathbf{d})$. Either of these two quantities may be larger, depending on whether the direction of $\mathbf{m}$ is noisier or quieter than the direction of $\mathbf{d}$. Because of its dependence on $\cos^2(\mathbf{m},\mathbf{d})$, the signal response is relatively insensitive to small mismatch between $\mathbf{m}$ and $\mathbf{d}$.

B. Noise-Alone Matrix Inverse ($\mathbf{k}_2=\mathbf{Q}^{-1}\mathbf{m}/\mathbf{m}^*\mathbf{Q}^{-1}\mathbf{m}$)

For the optimum beamformer based on inversion of the noise-alone cross-spectral matrix, substituting from Eq. 9 into Eq. 7 results in the following expression for array gain:

$$G(\mathbf{k}_2)=|\mathbf{m}^*\mathbf{Q}^{-1}\mathbf{d}|^2/(\mathbf{m}^*\mathbf{Q}^{-1}\mathbf{m}) =\mathbf{d}^*\mathbf{Q}^{-1}\mathbf{d}\cos^2(\mathbf{m},\mathbf{d};\mathbf{Q}^{-1}). \quad (27)$$

Again, the array gain depends on the cosine squared of a generalized angle between $\mathbf{m}$ and $\mathbf{d}$, but this time it is the angle in the space $H(\mathbf{Q}^{-1})$, where the metric is the inverse of the noise cross-spectral matrix. Notice that Eq. 27 reduces to Eq. 25 for the case of spatially uncorrelated noise $\mathbf{Q}=\mathbf{I}$. When $\mathbf{m}$ and $\mathbf{d}$ are perfectly matched, Eq. 27 reduces to Eq. 11.

The output spectrum of this beamformer is given by the following expression obtained by substituting from Eq. 9 into Eq. 5:

$$z(\mathbf{k}_2)=\sigma_1^2\{(\mathbf{d}^*\mathbf{Q}^{-1}\mathbf{d})/(\mathbf{m}^*\mathbf{Q}^{-1}\mathbf{m})\}\cos^2(\mathbf{m},\mathbf{d};\mathbf{Q}^{-1}) +\sigma_0^2/(\mathbf{m}^*\mathbf{Q}^{-1}\mathbf{m}). \quad (28)$$

The first term in Eq. 28 is the signal response and the second term is the noise response. Two distinct effects of the metric $\mathbf{Q}^{-1}$ on the signal response are evident. First is the effect of $\mathbf{Q}^{-1}$ on the angular separation between $\mathbf{m}$ and $\mathbf{d}$ manifested through the quantity $\cos^2(\mathbf{m},\mathbf{d};\mathbf{Q}^{-1})$. The angular separation and hence sensitivity to mismatch may be either larger or smaller in $H(\mathbf{Q}^{-1})$ than in $H(\mathbf{I})$, depending on how the metric $\mathbf{Q}^{-1}$ alters the vector space in the vicinity of $\mathbf{d}$. For example, if the eigenvalues of $\mathbf{Q}$ had considerable spread and if $\mathbf{d}$ nearly corresponded to an eigenvector associated with a large eigenvalue of $\mathbf{Q}$, then the optimum processor would usually be more sensitive to mismatch than the conventional processor, since differences in small projections of $\mathbf{m}$ and $\mathbf{d}$ on eigenvectors associated with small eigenvalues of $\mathbf{Q}$ would be emphasized by the metric $\mathbf{Q}^{-1}$. The second effect of the metric $\mathbf{Q}^{-1}$ on the signal response is manifested in the ratio $\{(\mathbf{d}^*\mathbf{Q}^{-1}\mathbf{d})/(\mathbf{m}^*\mathbf{Q}^{-1}\mathbf{m})\}$, which is the ratio of the length squared of $\mathbf{d}$ to the length squared of $\mathbf{m}$ in $H(\mathbf{Q}^{-1})$. Either of these two "lengths" may be the larger, depending on which corresponds to the quieter direction. The ratio may also be interpreted as the ratio of the maximum possible gain for the true signal direction to the maximum possible gain for the assumed signal direction.

C. Signal-plus-Noise Matrix Inverse ($\mathbf{k}_3=\mathbf{R}^{-1}\mathbf{m}/\mathbf{m}^*\mathbf{R}^{-1}\mathbf{m}$)

The array gain of the beamformer based on inversion of the signal-plus-noise cross-spectral matrix is given by the following equation obtained by substituting from Eq. 10 into Eq. 7:

$$G(\mathbf{k}_3)=|\mathbf{m}^*\mathbf{R}^{-1}\mathbf{d}|^2/(\mathbf{m}^*\mathbf{R}^{-1}\mathbf{Q}\mathbf{R}^{-1}\mathbf{m}). \quad (29)$$

Using Eqs. 22 and 23, this may be rewritten as

$$G(\mathbf{k}_3)=\frac{\mathbf{d}^*\mathbf{Q}^{-1}\mathbf{d}\cos^2(\mathbf{m},\mathbf{d};\mathbf{Q}^{-1})}{1+[2(\mathrm{S/N})_{max}+(\mathrm{S/N})_{max}^2]\sin^2(\mathbf{m},\mathbf{d};\mathbf{Q}^{-1})}. \quad (30)$$

The numerator of Eq. 30 may be recognized as $G(\mathbf{k}_2)$, the array gain of the beamformer based on inversion of the noise-alone cross-spectral matrix given in Eq. 27. Thus, the quantity in the denominator of Eq. 30,

$$G(\mathbf{k}_2)/G(\mathbf{k}_3)=1+[2(\mathrm{S/N})_{max}+(\mathrm{S/N})_{max}^2] \times\sin^2(\mathbf{m},\mathbf{d};\mathbf{Q}^{-1}), \quad (31)$$

gives the effect on array gain and output signal-to-noise ratio of including the signal in the matrix inversion process. Equation 31 is an important result with many practical implications.

Figure 2 presents plots of the gain ratio $G(\mathbf{k}_2)/G(\mathbf{k}_3)$ versus $\sin^2(\mathbf{m},\mathbf{d};\mathbf{Q}^{-1})$ for various values of $(\mathrm{S/N})_{max}$. Because the gain ratio depends on $(\mathrm{S/N})_{max}^2\sin^2(\mathbf{m},\mathbf{d};\mathbf{Q}^{-1})$, mismatch can cause a dramatic signal suppression when $(\mathrm{S/N})_{max}$ is greater than unity. For example, when $(\mathrm{S/N})_{max}=10$, and $\sin^2(\mathbf{m},\mathbf{d};\mathbf{Q}^{-1})=\cos^2(\mathbf{m},\mathbf{d};\mathbf{Q}^{-1})=0.5$, the gain ratio $G(\mathbf{k}_2)/G(\mathbf{k}_3)=61$. Then, the output signal-to-noise ratio of the $\mathbf{k}_2$-beamformer is $(0.5)(\mathrm{S/N})_{max}=5.0$, while the output signal-to-noise ratio of the $\mathbf{k}_3$-beamformer is $(5.0)/(61)=0.082$. The reduction is nearly 18 dB. If $(\mathrm{S/N})_{max}$ had been 2 instead of 10, the output signal-to-noise ratios of the $\mathbf{k}_2$ and $\mathbf{k}_3$ beamformers would have been 1 and 0.2, respectively. It is particularly significant that mismatch in the $\mathbf{k}_3$-beamformer can cause strong signals to be suppressed to such an extent that they have smaller output signal-to-noise ratios than weak signals with comparable mismatch. Also shown in Fig. 2 is the contour $G(\mathbf{k}_2)/G(\mathbf{k}_3)=(\mathrm{S/N})_{max}$. This locus is of interest because when $G(\mathbf{k}_2)/G(\mathbf{k}_3)\geq(\mathrm{S/N})_{max}$, the output signal-to-noise ratio of the $\mathbf{k}_3$-processor will be less than unity. For

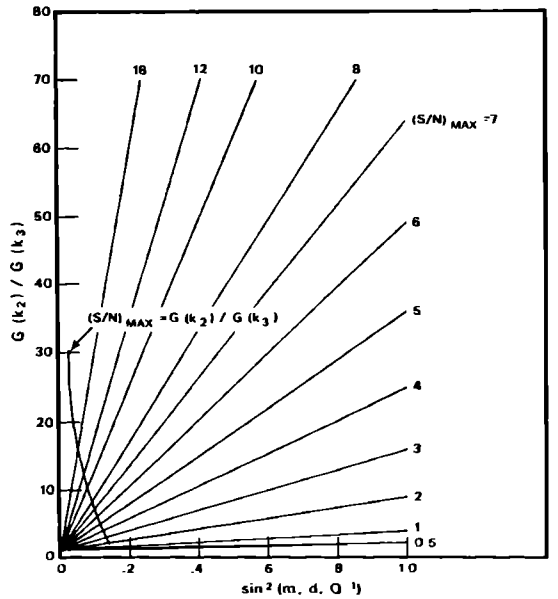

FIG. 2. Ratio of array gains $G(\mathbf{k}_3)/G(\mathbf{k}_2)$ vs amount of mismatch for various maximum possible output signal-to-noise ratios.

example, when $(S/N)_{max}=6$, the output signal-to-noise ratio of the $\mathbf{k}_3$-beamformer will be less than unity unless $\sin^2(\mathbf{m},\mathbf{d};\mathbf{Q}^{-1})$ is less than about 0.1.

From Eq. 31 it is evident that signal suppression cannot be large when $(S/N)_{max}$ is less than unity. However, values of $(S/N)_{max}$ larger than unity, when signal suppression can be a major problem, can correspond to small values of the input signal-to-noise ratio (σ_1^2/σ_0^2), especially when M is large.

One practical implication of Eq. 31 is that a $\mathbf{k}_3$-processor requires more closely spaced beams than a $\mathbf{k}_2$-, or $\mathbf{k}_1$-processor in order to avoid serious signal suppression effects being introduced on signals arriving from directions between the beams. Recalling that $\cos^2(\mathbf{m},\mathbf{d})$ is simply the beampattern of the conventional beamformer, suitable beam spacings can be obtained from Fig. 2 for anticipated values of $(S/N)_{max}$ for the case $\mathbf{Q}=\mathbf{I}$. To put the situation in perspective, we observe that the 3-dB down points on the main lobe response of a conventional beamformer correspond to $\sin^2(\mathbf{m},\mathbf{d})=0.5$.

Signal-to-noise ratio is not the only measure of performance. The behavior of the output is also of interest. Since the output spectrum of this beamformer is given by Eq. 13, the following expression for $z(\mathbf{k}_3)$ may be obtained by taking the reciprocal of Eq. 21:

$$z(\mathbf{k}_3)=\frac{\{\sigma_0^2/(\mathbf{m}^*\mathbf{Q}^{-1}\mathbf{m})\}\{1+(S/N)_{max}\}}{\{1+(S/N)_{max}\sin^2(\mathbf{m},\mathbf{d};\mathbf{Q}^{-1})\}}. \quad (32)$$

The effect of mismatch on the output spectrum may be seen more directly by examining the ratio of the output spectrums for the mismatched and perfectly matched $\mathbf{k}_3$-processor:

$$\frac{z(\mathbf{k}_3;\mathbf{m}\neq\mathbf{d})}{z(\mathbf{k}_3;\mathbf{m}=\mathbf{d})}=\{(\mathbf{d}^*\mathbf{Q}^{-1}\mathbf{d})/(\mathbf{m}^*\mathbf{Q}^{-1}\mathbf{m})\}\times\{1+(S/N)_{max}\sin^2(\mathbf{m},\mathbf{d};\mathbf{Q}^{-1})\}^{-1}. \quad (33)$$

In Eq. 33 we again see two distinct effects of mismatch. First is the effect of the ratio $\{(\mathbf{d}^*\mathbf{Q}^{-1}\mathbf{d})/\mathbf{m}^*\mathbf{Q}^{-1}\mathbf{m})\}$ which was discussed earlier, following Eq. 28. Second is the direct effect of mismatch embodied in the quantity $\{1+(S/N)_{max}\sin^2(\mathbf{m},\mathbf{d};\mathbf{Q}^{-1})\}^{-1}$. Notice that the effect of mismatch on the output spectrum depends on $(S/N)_{max}\sin^2(\mathbf{m},\mathbf{d};\mathbf{Q}^{-1})$ and not $(S/N)_{max}^2\times\sin^2(\mathbf{m},\mathbf{d};\mathbf{Q}^{-1})$ as did the effect on the output signal-to-noise ratio. From Eq. 32 it is apparent that increasing the signal strength and thereby increasing $(S/N)_{max}$ will always cause an increase in $z(\mathbf{k}_3)$ unless $\sin^2(\mathbf{m},\mathbf{d};\mathbf{Q}^{-1})$ is equal to 1. While this increase will be small when $(S/N)_{max}\sin^2(\mathbf{m},\mathbf{d};\mathbf{Q}^{-1})\gg 1$, the effect is unlike the effect on the output signal-to-noise ratio, where weak signals could lead to higher output signal-to-noise ratios than strong signals.

This apparent discrepancy can be clarified by obtaining an expression for $z(\mathbf{k}_3)$ which shows the effects of mismatch on the signal and noise responses individually. Such an alternative expression for $z(\mathbf{k}_3)$ may be obtained by rewriting Eq. 13 as follows:

$$z(\mathbf{k}_3)=\mathbf{m}^*\mathbf{R}^{-1}[\sigma_0^2\mathbf{Q}+\sigma_1^2\mathbf{d}\mathbf{d}^*]\mathbf{R}^{-1}\mathbf{m}/(\mathbf{m}^*\mathbf{R}^{-1}\mathbf{m})^2$$

or

$$z(\mathbf{k}_3)=\sigma_0^2\{\mathbf{m}^*\mathbf{R}^{-1}\mathbf{Q}\mathbf{R}^{-1}\mathbf{m}/(\mathbf{m}^*\mathbf{R}^{-1}\mathbf{m})^2\}+\sigma_1^2|\mathbf{m}^*\mathbf{R}^{-1}\mathbf{d}|^2/(\mathbf{m}^*\mathbf{R}^{-1}\mathbf{m})^2. \quad (34)$$

Substituting for $\mathbf{m}^*\mathbf{R}^{-1}\mathbf{m}$, $\mathbf{m}^*\mathbf{R}^{-1}\mathbf{Q}\mathbf{R}^{-1}\mathbf{m}$, and $|\mathbf{m}^*\mathbf{R}^{-1}\mathbf{d}|^2$ in Eq. 34 from Eqs. 21, 22, and 23 yields

$$z(\mathbf{k}_3)=\sigma_1^2\left(\frac{\mathbf{d}^*\mathbf{Q}^{-1}\mathbf{d}}{\mathbf{m}^*\mathbf{Q}^{-1}\mathbf{m}}\right)\times\frac{\cos^2(\mathbf{m},\mathbf{d};\mathbf{Q}^{-1})}{\{1+(S/N)_{max}\sin^2(\mathbf{m},\mathbf{d};\mathbf{Q}^{-1})\}^2}+\frac{\sigma_0^2}{\mathbf{m}^*\mathbf{Q}^{-1}\mathbf{m}}\times\left\{\frac{1+[2(S/N)_{max}+(S/N)_{max}^2]\sin^2(\mathbf{m},\mathbf{d};\mathbf{Q}^{-1})}{[1+(S/N)_{max}\sin^2(\mathbf{m},\mathbf{d};\mathbf{Q}^{-1})]^2}\right\}. \quad (35)$$

While Eq. 35 is considerably more complicated than Eq. 32, it does present explicit expressions for the signal response (first term in Eq. 35) and the noise response (second term in Eq. 35). By comparing these terms with the corresponding terms of Eq. 28, the effects of including the signal in the matrix inversion process may be perceived directly. Most interesting is the factor in large braces which multiples the average input noise power spectral level σ_0^2 in Eq. 35. The quantity in the numerator of this factor differs from the quantity in the denominator in that the numerator contains the

term $(S/N)_{max}^2 \sin^2(\mathbf{m},\mathbf{d};\mathbf{Q}^{-1})$ in place of the term $(S/N)_{max}^2 \sin^4(\mathbf{m},\mathbf{d};\mathbf{Q}^{-1})$ in the denominator. Thus, the factor is always equal to or greater than unity, with it being equal to unity only when $\sin^2(\mathbf{m},\mathbf{d};\mathbf{Q}^{-1})$ is equal to zero or 1. Hence, the noise response of the $\mathbf{k}_3$-beamformer is a function of the amount of mismatch. The nature of the noise response can be seen more easily by considering the case $\mathbf{Q}=\mathbf{I}$ so that the quantity $\mathbf{m}^*\mathbf{Q}^{-1}\mathbf{m}$ is constant. Then, as $\sin^2(\mathbf{m},\mathbf{d})$ is varied from zero to 1, the noise response increases from the value σ_0^2/M at $\sin^2(\mathbf{m},\mathbf{d})=0$ until it attains a maximum of $(\sigma_0^2/M)[2+(S/N)_{max}][4+4(S/N)_{max}]^{-1}$ at $\sin^2(\mathbf{m},\mathbf{d})=[2+(S/N)_{max}]^{-1}$ and then decreases until it again reaches the value (σ_0^2/M) at $\sin^2(\mathbf{m},\mathbf{d})=1$. One explanation of this unusual behavior of the noise response is that the $\mathbf{k}_3$-beamformer treats the mismatched signal as an unwanted interference and performs a compromise between suppressing it and rejecting the real noise. The stronger the mismatched signal, the more importance the processor puts on suppressing it. In suppressing the mismatched signal it accepts a lesser rejection of the noise. Near the point $\sin^2(\mathbf{m},\mathbf{d})=0$, the constraint $\mathbf{k}^*\mathbf{m}=1$ inhibits the suppression of the signal. As $\sin^2(\mathbf{m},\mathbf{d})$ is increased, the effect of the constraint decreases so that greater suppression of the signal is possible with a corresponding increased penalty in noise response. Eventually, the mismatch reaches the point where the signal suppression is sufficient that a further penalty in noise response is not justified. The processor then reverses the trend and places greater emphasis on rejecting the noise.

The increase in the noise response partially offsets the effect of the signal suppression on the output $z(\mathbf{k}_3)$. However, these two effects work together in decreasing the output signal-to-noise ratio.

Care should be taken in applying these asymptotic results to systems which adapt their parameters based on real-time measurements. The derivation of Expression 32 for $z(\mathbf{k}_3)$ involves a cancellation of field and filter parameters as can be seen in Eq. 13. Hence Eq. 32 does not allow for any change in the field which is not compensated for by a corresponding change in the filter vector $\mathbf{k}_3$. The same sort of cancellation is implicit in the use of the estimator $(\mathbf{m}^*\hat{\mathbf{R}}^{-1}\mathbf{m})^{-1}$. However, Eqs. 30 and 35 do not involve this type of cancellation. For example, suppose that the filter $\mathbf{k}_3$ was based on a cross-spectral matrix $\mathbf{R}_{T_1}$ measured during a particular time interval T_1 when the input signal and noise levels were $\bar{\sigma}_1^2$ and $\bar{\sigma}_0^2$ so that

$$\mathbf{R}_{T_1}=\bar{\sigma}_0^2\mathbf{Q}+\bar{\sigma}_1^2\mathbf{d}\mathbf{d}^*.$$

If the filter vector $\mathbf{k}_3$ which was determined from $\mathbf{R}_{T_1}$ were subsequently applied at a later time T_2 when the signal and noise levels were different so that

$$\mathbf{R}_{T_2}=\sigma_0^2\mathbf{Q}+\sigma_1^2\mathbf{d}\mathbf{d}^*,$$

then Eqs. 30 and 35 properly describe the array gain and output provided that $(S/N)_{max}$ in these equations is defined in terms of the signal-to-noise ratio $(\bar{\sigma}_1^2/\bar{\sigma}_0^2)$ used in determining $\mathbf{k}_3$.

Another view of the effect on the output spectrum of including the signal in the matrix inversion can be obtained by examining the ratio $z(\mathbf{k}_2)/z(\mathbf{k}_3)$. Dividing Eq. 28 by Eq. 32 and rearranging yields the following:

$$\frac{z(\mathbf{k}_2)}{z(\mathbf{k}_3)}=1+\frac{(S/N)_{max}^2 \sin^2(\mathbf{m},\mathbf{d};\mathbf{Q}^{-1})\cos^2(\mathbf{m},\mathbf{d};\mathbf{Q}^{-1})}{1+(S/N)_{max}}. \quad (36)$$

The interpretation of Eq. 36 may be simplified through the use of the trigonometric identity

$$\sin^2 a \cos^2 a=(1/4)\sin^2(2a). \quad (37)$$

Thus Eq. 36 may be written as

$$\frac{z(\mathbf{k}_2)}{z(\mathbf{k}_3)}=1+\frac{(S/N)_{max}^2 \sin^2[2(\mathbf{m},\mathbf{d};\mathbf{Q}^{-1})]}{4[1+(S/N)_{max}]}, \quad (38)$$

where Eq. 37 serves as the definition of $\sin^2[2(\mathbf{m},\mathbf{d};\mathbf{Q}^{-1})]$. From Eqs. 36 and 38 it is apparent that the level of the output spectrum of the $\mathbf{k}_2$-beamformer will be equal to or greater than that of the $\mathbf{k}_3$-beamformer. The two are equal only when there is perfect match $(\mathbf{m}=\mathbf{d})$ or when $\mathbf{m}$ and $\mathbf{d}$ are orthogonal in $H(\mathbf{Q}^{-1})$, $(|\mathbf{m}^*\mathbf{Q}^{-1}\mathbf{d}|^2=0)$. The relative behavior of the two beamformers as $\mathbf{m}$ is scanned in the vicinity of $\mathbf{d}$ may be determined from Eq. 38. As $\mathbf{m}$ is scanned through the set Ω of interest it will pass through some position of best match to $\mathbf{d}$ in the sense that $\cos^2(\mathbf{m},\mathbf{d};\mathbf{Q}^{-1})$ will achieve a local maximum. The maximum value may be less than unity since $\mathbf{d}$ may not correspond exactly to any of the steering vectors in the set through which $\mathbf{m}$ is scanned. From Eq. 38 we see that if the angle between $\mathbf{m}$ and $\mathbf{d}$ in $H(\mathbf{Q}^{-1})$ at the point of best match is sufficiently small, the ratio $z(\mathbf{k}_2)/z(\mathbf{k}_3)$ will initially increase as the angle is increased by scanning $\mathbf{m}$ away from the point of best match. This initial increase in $z(\mathbf{k}_2)/z(\mathbf{k}_3)$ means that the output of the $\mathbf{k}_3$-processor is decreasing more rapidly than that of the $\mathbf{k}_2$-processor and hence the peak on the output of the $\mathbf{k}_3$-processor will be sharper than that of the $\mathbf{k}_2$-processor. The condition that the angle between $\mathbf{m}$ and $\mathbf{d}$ be sufficiently small at the position of best match may be expressed as

$$\max_{\mathbf{m}\in\Omega} \cos^2(\mathbf{m},\mathbf{d};\mathbf{Q}^{-1})>\tfrac{1}{2}. \quad (39)$$

Whenever Expression 39 is satisfied, the peak in the scanned output of the $\mathbf{k}_3$-processor will be sharper than that of the $\mathbf{k}_2$-processor. Conversely, if

$$\max_{\mathbf{m}\in\Omega} \cos^2(\mathbf{m},\mathbf{d};\mathbf{Q}^{-1})<\tfrac{1}{2}, \quad (40)$$

$z(\mathbf{k}_2)/z(\mathbf{k}_3)$ will initially decrease and the $\mathbf{k}_2$-processor will have the sharper peak in its scanned response.

The preceding argument concerning the ratio $z(\mathbf{k}_2)/z(\mathbf{k}_3)$ and the relative sharpness of the peaks in the scanned outputs generalizes a result of Seligson,[14] who compared $z(\mathbf{k}_1)/z(\mathbf{k}_3)$ for the case of spatially uncorrelated noise so that $z(\mathbf{k}_2)$ and $z(\mathbf{k}_1)$ coincided. He derived an expression equivalent to Eq. 36 in that case and presented the argument concerning the relative sharpness of the peaks.

A simple expression for $z(\mathbf{k}_3)$ which will be useful in later discussions may be obtained by substituting from Eq. 19 into Eq. 3:

$$z(\mathbf{k}_3)=\{\mathbf{m}^*[\sigma_0^2\mathbf{Q}+\sigma_1^2\mathbf{dd}^*]^{-1}\mathbf{m}\}^{-1}. \quad (41)$$

IV. RESOLUTION

The classical concept of resolution consists of recognizing that an observed effect is due to two separate sources rather than a single source. High resolution is the ability to separate the effects of two closely spaced sources. In this section we will consider primarily the resolving power of the $\mathbf{k}_3$-beamformer. Some results will be presented for the conventional $\mathbf{k}_1$-beamformer to provide a basis for comparison.

A. Qualitative Discussion

Before determining exact conditions for resolution it is worthwhile to use the results already obtained concerning mismatch in considering the simpler problem of determining the effect of one source on the output of a $\mathbf{k}_3$-beamformer which is perfectly matched to a second source. Let

$$\mathbf{R}=\sigma_0^2\mathbf{Q}+\sigma_1^2\mathbf{dd}^*+\sigma_2^2\mathbf{bb}^*, \quad (42)$$

where $\mathbf{d}$ and $\mathbf{b}$ are the direction vectors for the first and second sources, respectively. When the beamformer is perfectly matched to $\mathbf{b}$, it follows from Eq. 32 that its output spectrum is given by the following equation:

$$z_b=[\mathbf{b}^*\mathbf{R}^{-1}\mathbf{b}]^{-1}=\sigma_2^2+\{\mathbf{b}^*[\sigma_0^2\mathbf{Q}+\sigma_1^2\mathbf{dd}^*]^{-1}\mathbf{b}\}^{-1}. \quad (43)$$

The subscript b on z_b is a reminder that the processor is perfectly matched to $\mathbf{b}$, that is, $\mathbf{k}_3=\mathbf{R}^{-1}\mathbf{b}/(\mathbf{b}^*\mathbf{R}^{-1}\mathbf{b})$.

The first term in Eq. 43 is due to the $\mathbf{b}$-component which passes through the beamformer without distortion. The second term is the combined result of the noise and the $\mathbf{d}$-component. If $\mathbf{m}$ in Eq. 41 is replaced with $\mathbf{b}$, the second term in Eq. 43 becomes identical to Eq. 41. Thus the results developed earlier for a single source with a mismatched $\mathbf{k}_3$-beamformer may be applied directly to the case of two sources with the beamformer perfectly matched to one of them.

For example, defining

$$(S_1/N)_{max}=\mathbf{d}^*\mathbf{Q}^{-1}\mathbf{d}\sigma_1^2/\sigma_0^2 \quad (44)$$

so that $(S_1/N)_{max}$ is the maximum output signal-to-noise ratio for the $\mathbf{d}$-component in the absence of the $\mathbf{b}$-component, the expression given in Eq. 32 may be substituted for the second term in Eq. 43, yielding

$$z_b=\sigma_2^2+\{\sigma_0^2/(\mathbf{b}^*\mathbf{Q}^{-1}\mathbf{b})\}\{1+(S_1/N)_{max}\}/\{1+(S_1/N)_{max}\sin^2(\mathbf{b},\mathbf{d};\mathbf{Q}^{-1})\}. \quad (45)$$

When the first term in Eq. 45 is much larger than the second, the output signal-to-background ratio for the $\mathbf{b}$-component is high when the processor is perfectly matched to $\mathbf{b}$.

An alternate form of Eq. 45 may be obtained by adding $\sigma_0^2/(\mathbf{b}^*\mathbf{Q}^{-1}\mathbf{b})$ to the first term in Eq. 45 and compensating by subtracting it from the second term. Then Eq. 45 becomes

$$z_b=\{\sigma_2^2+\sigma_0^2/(\mathbf{b}^*\mathbf{Q}^{-1}\mathbf{b})\}+\frac{\sigma_0^2}{\mathbf{b}^*\mathbf{Q}^{-1}\mathbf{b}}\left\{\frac{(S_1/N)_{max}\cos^2(\mathbf{d},\mathbf{b};\mathbf{Q}^{-1})}{1+(S_1/N)_{max}\sin^2(\mathbf{d},\mathbf{b};\mathbf{Q}^{-1})}\right\}. \quad (46)$$

The term within the first pair of braces in Eq. 46 may be recognized as $\{\mathbf{b}^*[\sigma_0^2\mathbf{Q}+\sigma_2^2\mathbf{bb}^*]^{-1}\mathbf{b}\}^{-1}$, which is what the output would be in the absence of the $\mathbf{d}$-component. When this term is much larger than the second term in Eq. 46, the presence of the $\mathbf{d}$-component has little effect on the beamformer output. Defining

$$(S_2/N)_{max}=\mathbf{b}^*\mathbf{Q}^{-1}\mathbf{b}\sigma_2^2/\sigma_0^2,$$

the condition that the first term in Eq. 46 be much larger than the second term may be written as

$$1+(S_2/N)_{max}\gg\frac{(S_1/N)_{max}\cos^2(\mathbf{d},\mathbf{b};\mathbf{Q}^{-1})}{1+(S_1/N)_{max}\sin^2(\mathbf{d},\mathbf{b};\mathbf{Q}^{-1})}. \quad (47)$$

When $(S_1/N)_{max}\sin^2(\mathbf{b},\mathbf{d};\mathbf{Q}^{-1})>1$ this may be simplified to the following:

$$(S_2/N)_{max}\gg\frac{\cos^2(\mathbf{d},\mathbf{b};\mathbf{Q}^{-1})}{\sin^2(\mathbf{d},\mathbf{b};\mathbf{Q}^{-1})}=\cot^2(\mathbf{d},\mathbf{b};\mathbf{Q}^{-1}). \quad (48)$$

For the case $\mathbf{Q}=\mathbf{I}$, Capon[13] argues that, when the first source has little effect on the output of the $\mathbf{k}_3$-processor which is perfectly matched to the second source, the two sources will be resolved. He suggests a relationship equivalent to Eq. 48 and an analogous one for $(S_1/N)_{max}$ as criteria for resolution. A weakness in this argument is that it attempts to infer the behavior of the scanned processor output from only the magnitude of the two terms at the single point $\mathbf{m}=\mathbf{b}$. This, together with the imprecise nature of the "much greater than" type of condition makes desirable a more quantitative treatment of the resolution question.

In spite of the above remarks concerning their use as a basis of a resolution criterion, Eqs. 45 and 46 do provide useful information concerning the effect of one signal on the output of a $\mathbf{k}_3$-processor which is matched to the other. Another equivalent expression for z_b may be obtained by using Eq. 35 to replace the second term in Eq. 43 similarly to the way Eq. 32 was used in obtaining Eq. 45. Rather than pursue this straight-

forward substitution, we simply note that it provides explicit expressions for the contributions of the two signals and noise to the output.

B. Exact Conditions for Resolution

In developing exact conditions under which two components will be resolved by a $\mathbf{k}_3$-beamformer, we will consider the case of uncorrelated noise so that $\mathbf{Q}=\mathbf{I}$. This assumption will make the analysis slightly simpler and will avoid the necessity of stating restrictions on $\mathbf{Q}$ in order to avoid anomalous situations which are possible for a general $\mathbf{Q}$ matrix. For example, a general noise matrix $\mathbf{Q}$ could contain a third component between the two we are trying to resolve. The assumption of uncorrelated noise also avoids confusion between the super-gain phenomenon[16] which arises in the isotropic noise case and the resolution phenomenon which is our prime concern. We shall initially consider the case when the two components to be resolved are of equal strength. Resolution of signals of unequal strength is considered in a later section. Thus $\mathbf{R}$ is assumed to have the following form:

$$\mathbf{R}=\sigma_0^2\mathbf{I}+\sigma_1^2\mathbf{dd}^*+\sigma_1^2\mathbf{bb}^*. \tag{49}$$

From the symmetry of Eq. 49 it is evident that the output will be the same when $\mathbf{m}$ is perfectly matched to either $\mathbf{d}$ or $\mathbf{b}$.

In order to study the question of resolution, we shall compare the output spectrum when $\mathbf{m}$ is perfectly matched to one of the two signals with the output spectrum when $\mathbf{m}$ is steered to a value $\mathbf{m}_0$ which corresponds to a position midway between the two sources. Rather than work with the outputs directly, it is easier to work with the ratio

$$z_d/z_m=(\mathbf{m}^*\mathbf{R}^{-1}\mathbf{m})/(\mathbf{d}^*\mathbf{R}^{-1}\mathbf{d}), \tag{50}$$

where $\mathbf{R}$ is given by Eq. 49. An expression for this ratio may be obtained from the reciprocal of Eq. 33 by using $(\sigma_0^2\mathbf{I}+\sigma_1^2\mathbf{bb}^*)$ in place of $\sigma_0^2\mathbf{Q}$. This yields

$$z_d/z_m=\{\mathbf{m}^*[\sigma_0^2\mathbf{I}+\sigma_1^2\mathbf{bb}^*]^{-1}\mathbf{m}\}\times\{\mathbf{d}^*[\sigma_0^2\mathbf{I}+\sigma_1^2\mathbf{bb}^*]^{-1}\mathbf{d}\}^{-1}\{1+\sigma_1^2\mathbf{d}^*[\sigma_0^2\mathbf{I}+\sigma_1^2\mathbf{bb}^*]^{-1}\mathbf{d}\times\sin^2(\mathbf{m},\mathbf{d};[\sigma_0^2\mathbf{I}+\sigma_1^2\mathbf{bb}^*]^{-1})\}. \tag{51}$$

After considerable algebraic manipulation (shown in Appendix B), Eq. 51 may be reduced to the following simplified form:

$$z_d/z_m=\{1+(M\sigma_1^2/\sigma_0^2)[1-\cos^2(\mathbf{m},\mathbf{b})-\cos^2(\mathbf{m},\mathbf{d})-\alpha\cos^2(\mathbf{d},\mathbf{b})+(2\alpha/M^3)\,\mathrm{Re}(\mathbf{m}^*\mathbf{dd}^*\mathbf{bb}^*\mathbf{m})]\}\times\{1-\alpha\cos^2(\mathbf{d},\mathbf{b})\}^{-1}, \tag{52}$$

where $\mathrm{Re}(\cdot)$ denotes the real part and α is defined as follows:

$$\alpha=\frac{(M\sigma_1^2/\sigma_0^2)}{(1+M\sigma_1^2/\sigma_0^2)}. \tag{53}$$

Notice that $M\sigma_1^2/\sigma_0^2$ is the maximum output signal-to-noise ratio for either source in the absence of the other. In this case ($\mathbf{Q}=\mathbf{I}$), $M\sigma_1^2/\sigma_0^2$ is the output signal-to-noise ratio for either source of a perfectly matched conventional beamformer in the absence of the other source. The parameter α is nearly unity when $M\sigma_1^2/\sigma_0^2\gg1$.

An important simplification occurs when $\mathbf{m}$, $\mathbf{b}$, and $\mathbf{d}$ are direction vectors corresponding to plane waves and the array is composed of symmetric pairs of sensors. In this case $(\mathbf{m}^*\mathbf{d})$, $(\mathbf{d}^*\mathbf{b})$, and $(\mathbf{b}^*\mathbf{m})$ are all real. Then, since $(\mathbf{m}^*\mathbf{m})$, $(\mathbf{b}^*\mathbf{b})$, and $(\mathbf{d}^*\mathbf{d})$ are all normalized to be equal to M, we can define

$$\cos(\mathbf{m},\mathbf{b})=(\mathbf{m}^*\mathbf{b})/M, \quad \text{for } (\mathbf{m}^*\mathbf{b}) \text{ real}, \tag{54}$$

consistent with the definition of $\cos^2(\mathbf{m},\mathbf{b})$. Then

$$(2\alpha/M^3)\,\mathrm{Re}(\mathbf{m}^*\mathbf{dd}^*\mathbf{bb}^*\mathbf{m})=2\alpha\cos(\mathbf{m},\mathbf{d})\cos(\mathbf{d},\mathbf{b})\cos(\mathbf{b},\mathbf{m}) \tag{55}$$

and Eq. 52 becomes

$$z_d/z_m=\{1+(M\sigma_1^2/\sigma_0^2)[1-\cos^2(\mathbf{m},\mathbf{b})-\cos^2(\mathbf{m},\mathbf{d})-\alpha\cos^2(\mathbf{d},\mathbf{b})+2\alpha\cos(\mathbf{m},\mathbf{d})\cos(\mathbf{d},\mathbf{b})\cos(\mathbf{m},\mathbf{b})]\}\times\{1-\alpha\cos^2(\mathbf{d},\mathbf{b})\}^{-1}. \tag{56}$$

In order to study the question of resolution, we examine the ratio (z_d/z_m) when $\mathbf{m}$ is equal to $\mathbf{m}_0$ which is the midpoint between $\mathbf{b}$ and $\mathbf{d}$ in the sense that

$$\cos^2(\mathbf{m}_0,\mathbf{b})=\cos^2(\mathbf{m}_0,\mathbf{d}). \tag{57}$$

Substituting from Eq. 57 into Eq. 56 gives the following surprisingly simple expression for (z_d/z_{m_0}) for plane wave signals and pairwise symmetric arrays:

$$z_d/z_{m_0}=\frac{1+(M\sigma_1^2/\sigma_0^2)\{1-\alpha\cos^2(\mathbf{d},\mathbf{b})-2\cos^2(\mathbf{m}_0,\mathbf{b})[1-\alpha\cos(\mathbf{d},\mathbf{b})]\}}{1-\alpha\cos^2(\mathbf{d},\mathbf{b})}. \tag{58}$$

Equation 58 provides the basis for determining the ability of pairwise symmetric arrays to resolve plane wave components. If $(z_d/z_{m_0})<1$, the response at the midpoint is greater than at either of the signal directions and the effects of the two sources have merged into a single peak in the scanned output. When

$$(z_d/z_{m_0})>1, \tag{59}$$

the response at the "midpoint" is less than at either of the "on-target" directions and we shall say that

signals are resolved. Moreover, Eq. 58 enables us to determine the depth of "valley" between the peaks associated with the resolved signals.

In practice, it may be desirable to set a slightly higher threshold on the minimum (z_d/z_{m_0}) for which signals will be called resolved, so that the "valley" is easily seen. However, unlike Expression 59, the setting of such a higher threshold is rather arbitrary. For example, $(z_d/z_{m_0})=\pi^2/8\approx 1.23$ corresponds to the classical Rayleigh limit for a line array, but the value of (z_d/z_{m_0}) at the Rayleigh limit is different for different geometries.[20]

Recalling that $\cos^2(\cdot,\cdot)$ may be interpreted as the beam pattern of the array with a conventional beamformer, it is seen that Eq. 58 provides the exact resolution information of the optimum $\mathbf{k}_3$-processor explicitly in terms of conventional beam patterns and the output signal-to-noise ratio $(M\sigma_1^2/\sigma_0^2)$ of a perfectly matched conventional beamformer with only one source present.

In the absence of the pairwise symmetry and plane wave assumptions, Eq. 57 may still be used in Eq. 52. Then

$$z_d/z_{m_0}=\{1+(M\sigma_1^2/\sigma_0^2)[1-\alpha\cos^2(\mathbf{d},\mathbf{b})-2\cos^2(\mathbf{m}_0,\mathbf{b}) +(2\alpha/M^3)\,\mathrm{Re}(\mathbf{m}_0^*\mathbf{d}\mathbf{d}^*\mathbf{b}\mathbf{b}^*\mathbf{m}_0)]\} \times\{1-\alpha\cos^2(\mathbf{d},\mathbf{b})\}^{-1}$$

may be used in Expression 59 as the condition for resolution. Noting that

$$\mathrm{Re}(\mathbf{m}_0^*\mathbf{d}\mathbf{d}^*\mathbf{b}\mathbf{b}^*\mathbf{m}_0)\le|\mathbf{m}_0^*\mathbf{d}||\mathbf{d}^*\mathbf{b}||\mathbf{b}^*\mathbf{m}_0| =|\mathbf{m}_0\mathbf{d}|^2|\mathbf{d}^*\mathbf{b}| \quad (60)$$

or

$$(2\alpha/M^3)\,\mathrm{Re}(\mathbf{m}_0^*\mathbf{d}\mathbf{d}^*\mathbf{b}\mathbf{b}^*\mathbf{m}_0) \le 2\alpha\cos^2(\mathbf{m}_0,\mathbf{b})[\cos^2(\mathbf{d},\mathbf{b})]^{\frac{1}{2}}, \quad (61)$$

we obtain the following bound on z_d/z_{m_0}:

$$z_d/z_{m_0}\le\frac{1+(M\sigma_1^2/\sigma_0^2)(1-\alpha\cos^2(\mathbf{d},\mathbf{b})-2\cos^2(\mathbf{m}_0,\mathbf{b})\{1-\alpha[\cos^2(\mathbf{d},\mathbf{b})]^{\frac{1}{2}}\})}{1-\alpha\cos^2(\mathbf{d},\mathbf{b})}, \quad (62)$$

which closely resembles Eq. 58. The condition that the right side of Eq. 62 be greater than unity is clearly necessary for resolution.

C. Conventional Beamformer

For purposes of comparison it is useful to consider the corresponding resolution question for a conventional beamformer. When $\mathbf{R}$ is given by Eq. 49, the output spectrum of the conventional beamformer is

$$z(\mathbf{k}_1)=(\sigma_0^2/M)+\sigma_1^2\cos^2(\mathbf{m},\mathbf{b})+\sigma_1^2\cos^2(\mathbf{m},\mathbf{d}). \quad (63)$$

The ratio of "on-target" to "midpoint" response is

$$\frac{z_d(\mathbf{k}_1)}{z_{m_0}(\mathbf{k}_1)}=\frac{\mathbf{d}^*\mathbf{R}\mathbf{d}}{\mathbf{m}_0^*\mathbf{R}\mathbf{m}_0}=\frac{1+\cos^2(\mathbf{d},\mathbf{b})+(M\sigma_1^2/\sigma_0^2)^{-1}}{2\cos^2(\mathbf{m}_0,\mathbf{b})+(M\sigma_1^2/\sigma_0^2)^{-1}}. \quad (64)$$

The signal-to-noise ratio parameter $(M\sigma_1^2/\sigma_0^2)$ cannot alter the result whether or not $z_d(\mathbf{k}_1)/z_{m_0}(\mathbf{k}_1)$ is larger than unity. For $(M\sigma_1^2/\sigma_0^2)>1$, the ratio $z_d(\mathbf{k}_1)/z_{m_0}(\mathbf{k}_1)$ is quite insensitive to changes in $(M\sigma_1^2/\sigma_0^2)$.

From Eq. 64 a necessary and sufficient condition for resolution by a conventional beamformer is

$$[1+\cos^2(\mathbf{d},\mathbf{b})]/[2\cos^2(\mathbf{m}_0,\mathbf{b})]>1. \quad (65)$$

Condition 65 will be satisfied whenever

$$\cos^2(\mathbf{m}_0,\mathbf{b})<\tfrac{1}{2}, \quad (66)$$

so that Expression 66 is a sufficient condition for resolution by a conventional beamformer. Condition 66 simply states that resolution is guaranteed if the spacing of the sources is such that the response at "midpoint" steering from each source is more than 3 dB below the response for "on-target" steering.

D. Resolving Power of a Line Array

In this section the results of the preceding analysis are applied to an array of sensors uniformly distributed on a straight line.

The geometry of the line array example is shown in Fig. 3. Two targets are located in the farfield of the line array at small angles of $\theta/2$ and $-\theta/2$ from broadside, respectively. The length L of the array is at least several wavelengths and the sensors are spaced at intervals of less than $\lambda/2$, one-half the wavelength.

Under these conditions, the following approximate expressions relate the mathematical quantities $\cos^2(\mathbf{m}_0,\mathbf{b})$ and $\cos(\mathbf{d},\mathbf{b})$ to the physical quantities L, θ, and λ:

$$\cos(\mathbf{d},\mathbf{b})=\frac{\sin(\pi L\theta/\lambda)}{(\pi L\theta/\lambda)} \quad (67)$$

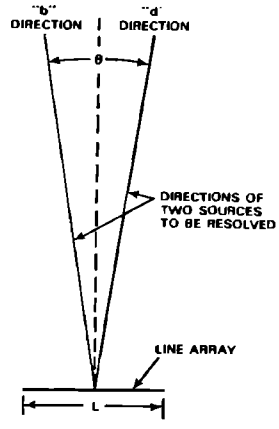

FIG. 3. Geometry of line array example.

and

$$\cos^2(\mathbf{m}_0,\mathbf{b})=\frac{\sin^2[\pi L(\theta/2)/\lambda]}{[\pi L(\theta/2)/\lambda]^2} \tag{68}$$

For this geometry, the classical Rayleigh resolution criterion for conventional beamforming is

$$\theta \geq \lambda/L. \tag{69}$$

The equality in Expression 69 holds when the separation of the two sources is such that one source is located at the position of the first null of the beampattern of a conventional beamformer steered at the second source. That is, using $\theta=\lambda/L$ in Eq. 67 gives $\cos(\mathbf{d},\mathbf{b})=0$. Using $\theta=\lambda/L$ in Eq. 68 gives $\cos^2(\mathbf{m}_0,\mathbf{b})=(2/\pi)^2=0.41$, which satisfies Expression 66. Using Eq. 64, we see that, when $M\sigma_1^2/\sigma_0^2 \gg 1$, the separation $\theta=\lambda/L$ yields a ratio of "on-target" to "midpoint" response of $z_d(\mathbf{k}_1)/z_{m_0}(\mathbf{k}_1)=(\pi^2/8)\approx 1.23$. Thus the Rayleigh limit is more than the bare minimum criterion of $z_d(\mathbf{k}_1)/z_{m_0}(\mathbf{k}_1)>1$. The quantity $(1/\theta)$ at the resolution limit is known as the resolving power of the system.[20] These classical results for conventional beamformers serve as a benchmark for the resolving power of the optimum $\mathbf{k}_3$-processor.

The ratio of "on-target" to "midpoint" response obtained by substituting from Eqs. 67 and 68 into 58 is plotted in Fig. 4, for various values of the signal-to-noise ratio parameter $M\sigma_1^2/\sigma_0^2$. Also shown is the same ratio for a conventional beamformer obtained by substituting from Eqs. 67 and 68 into Eq. 64 for large $M\sigma_1^2/\sigma_0^2$.

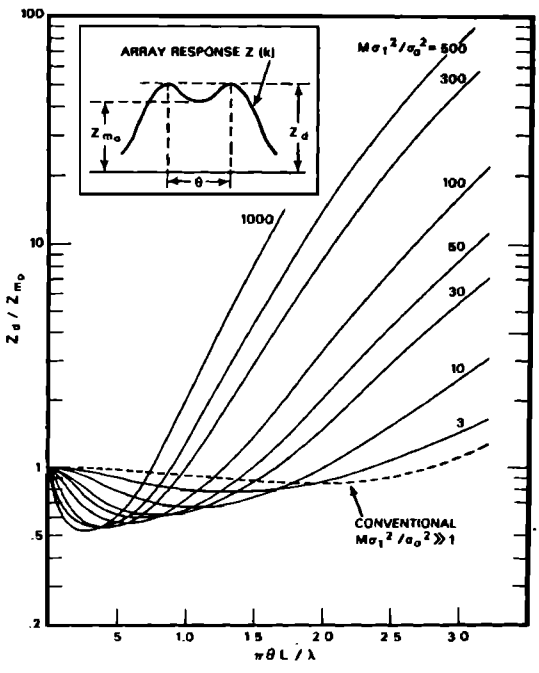

FIG. 4. Ratio of "on target" to "mid-point" response ratio of optimum ($\mathbf{k}_3$) beamformer on a line array for various values of the output signal-to-noise parameter $M\sigma_1^2/\sigma_0^2$ compared with a conventional ($\mathbf{k}_1$) beamformer.

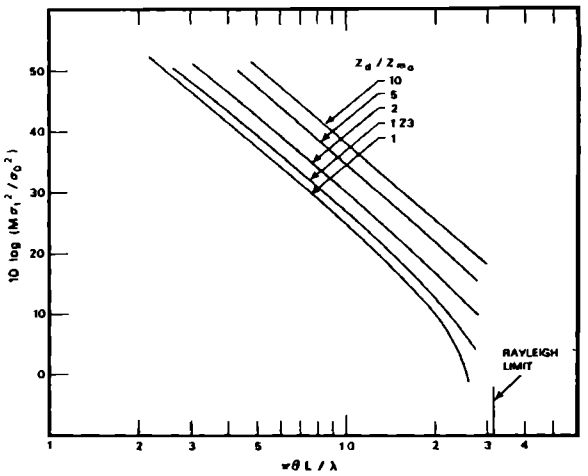

FIG. 5. Required value of the output signal-to-noise ratio parameter $M\sigma_1^2/\sigma_0^2$ versus normalized angular separation for resolution by a line array for various levels of the "on target" to "mid-point" response ratio.

The use of some value larger than unity for a minimum level of z_d/z_{m_0} for practical resolution is facilitated by the presentation of Fig. 4. A direct comparison with the classical Rayleigh limit may be made by using $z_d/z_{m_0}=1.23$. For example, when $M\sigma_1^2/\sigma_0^2=500$ or 27 dB, the $\mathbf{k}_3$-processor achieves the ratio $z_d/z_{m_0}=1.23$ at about $\theta=\lambda/(\pi L)$ compared with $\theta=\lambda/L$ for the conventional processor, and the $\mathbf{k}_3$-processor can be said to have slightly more than three times the resolving power of the conventional beamformer.

The effect of signal-to-noise ratio on resolution by the $\mathbf{k}_3$-processor may be seen more directly in Fig. 5, which presents the required value of $M\sigma_1^2/\sigma_0^2$ versus angular separation for various levels of z_d/z_{m_0}. From Fig. 5, it is apparent that increasing signal-to-noise ratio by about 13 dB improves the resolving power of the $\mathbf{k}_3$-processor by a factor of 2. For a fixed separation angle θ, Fig. 5 shows that the ratio z_d/z_{m_0} increases rapidly as the signal-to-noise ratio is increased. Thus the $\mathbf{k}_3$-processor will usually have clearly defined peaks in its response when the signal-to-noise ratio is slightly higher than that required for resolution.

E. Resolution of Signals of Unequal Strength

The case in which the two signals to be resolved are of unequal strength is somewhat more complicated than when they are of equal strength. Indeed, the very definition of resolution is subject to question. Three hypothetical scanned beamformer responses to two spatially separated sources plus noise are shown in Fig. 6. For the situation shown in Fig. 6(a) only a single peak is visible and it is obvious that the two sources are not resolved. For the situation shown in Fig. 6(c) there is a definite valley between two peaks of different

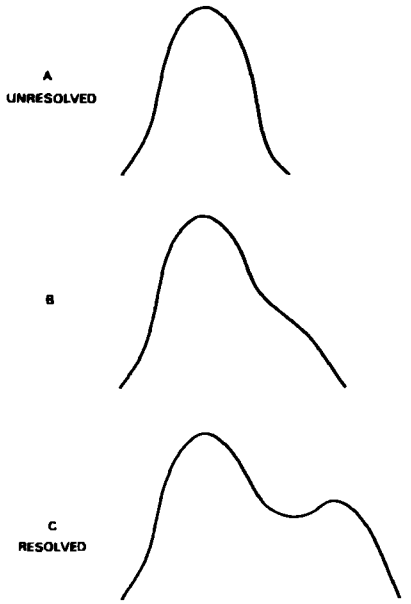

FIG. 6. Typical scanned beamformer responses to two unequal sources.

heights, and it is natural to say that the two sources are resolved. An intermediate situation is illustrated in Fig. 6(b), in which the presence of the weaker source alters the shape of the response due to the stronger source but no separate peak exists. The definition which we shall use for resolution will require a definite valley between the two peaks as in Fig. 6(c). Thus we shall say that in the situation shown in Fig. 6(b) the sources are not resolved.

Before proceeding, it is worthwhile to consider what the results already developed imply about the resolution of signals of unequal strength. Suppose that there are two sources of equal strength at some fixed separation. If the strength of the second source is increased, then from Eq. 32 the output $z(\mathbf{k}_3)$ will increase for all steering directions except those which are orthogonal in the appropriate space to the direction vector for that source. The amount of increase of the output depends on the sine squared of the generalized angle between the steering vector and the direction vector of the second source. The dependence is monotonic, so that the smaller the sine squared, the greater the increase in the output $z(\mathbf{k}_3)$. Thus, if the sine squared of that angle increases monotonically as the steering vector is scanned from the second source to the first source, then increasing the strength of the second source will cause an increase in the output for all steering directions between the two sources with the amount of increase being less for steering directions which are farther from the second source. In this situation, which is normal for closely spaced (within the Rayleigh limit) sources, a necessary condition for resolution is that the two sources were originally resolvable when the strength of the second source was equal to that of the weaker first source. Thus a necessary condition for resolution by a $\mathbf{k}_3$-beamformer of two closely unequal sources is that the two sources would be resolvable if both had the strength of the weaker source.

To be precise, let

$$\mathbf{R}=\sigma_0^2\mathbf{I}+\sigma_1^2\mathbf{dd}^*+\sigma_2^2\mathbf{bb}^*, \quad \sigma_2^2\geq\sigma_1^2, \tag{70}$$

and let

$$\mathbf{W}=\sigma_0^2\mathbf{I}+\sigma_1^2\mathbf{dd}^*. \tag{71}$$

If $\sin^2(\mathbf{m},\mathbf{b};\mathbf{W}^{-1})$ increases monotonically as $\mathbf{m}$ is scanned from $\mathbf{b}$ to $\mathbf{d}$, then a necessary condition for resolution is that the sources be resolvable when

$$\mathbf{R}=\sigma_0^2\mathbf{I}+\sigma_1^2\mathbf{dd}^*+\sigma_1^2\mathbf{bb}^*.$$

While the above condition is necessary for resolution, it is not sufficient, since increasing the strength of the second source could result in the situation depicted in Fig. 6(b). In order to develop a sufficient condition for resolution we shall proceed in a manner similar to that used for the case of signals of equal strength and consider the ratio z_d/z_m given by Eq. 50. Since $\mathbf{d}$ is the direction vector for the weaker source a value of z_d/z_m greater than unity at some point between $\mathbf{d}$ and $\mathbf{b}$ in the scanned response is necessary and sufficient for resolution. The following generalization of Eq. 52 for the situation in which $\mathbf{R}$ is given by Eq. 70 is derived in Appendix B:

$$\begin{aligned} z_d/z_m=\{1+(M\sigma_1^2/\sigma_0^2)[1-(\alpha_2/\alpha_1)\cos^2(\mathbf{m},\mathbf{b}) \\ -\cos^2(\mathbf{m},\mathbf{d})-\alpha_2\cos^2(\mathbf{d},\mathbf{b}) \\ +(2\alpha_2/M^3)\,\mathrm{Re}(\mathbf{m}^*\mathbf{dd}^*\mathbf{bb}^*\mathbf{m})]\} \\ \times\{1-\alpha_2\cos^2(\mathbf{d},\mathbf{b})\}^{-1}, \end{aligned} \tag{72}$$

where in analogy with Eq. 53

$$\alpha_i=\frac{(M\sigma_i^2/\sigma_0^2)}{(1+M\sigma_i^2/\sigma_0^2)}, \quad i=1,2. \tag{73}$$

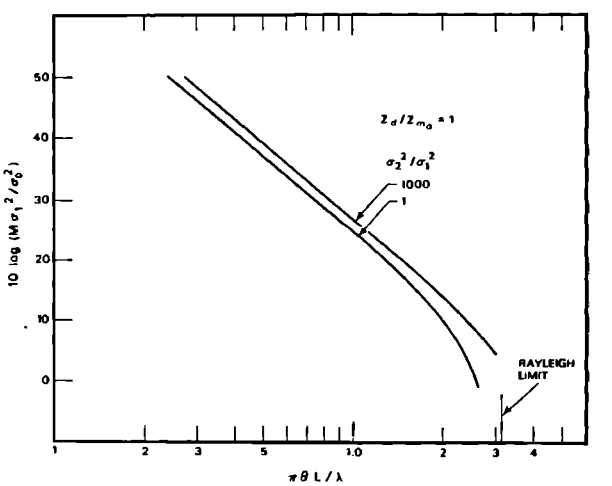

FIG. 7. Comparison of sufficient condition for resolution of unequal sources with a line array when $\sigma_2^2/\sigma_1^2=1000$ with the necessary condition.

For the case of plane waves and pairwise symmetric arrays, Eq. 72 reduces to the following generalization of Eq. 56:

$$z_d/z_m=\{1+(M\sigma_1^2/\sigma_0^2)[1-(\alpha_2/\alpha_1)\cos^2(\mathbf{m},\mathbf{b}) -\cos^2(\mathbf{m},\mathbf{d})-\alpha_2\cos^2(\mathbf{d},\mathbf{b}) +2\alpha_2\cos(\mathbf{m},\mathbf{d})\cos(\mathbf{d},\mathbf{b})\cos(\mathbf{m},\mathbf{b})]\} \times\{1-\alpha_2\cos^2(\mathbf{d},\mathbf{b})\}^{-1}. \quad (74)$$

Unlike the situation for signals of equal strength, we do not expect that when the two signals are resolved the largest value of z_d/z_m will occur at the midpoint $\mathbf{m}=\mathbf{m}_0$. Thus the condition

$$z_d/z_{m_0}>1 \quad (75)$$

used previously is not a necessary condition for resolution when the signals are of unequal strength, but it clearly is a sufficient condition for resolution. Substituting from Eq. 57 into Eq. 74 yields the following generalization of Eq. 58:

$$z_d/z_{m_0}=\frac{1+(M\sigma_1^2/\sigma_0^2)\{1-\alpha_2\cos^2(\mathbf{d},\mathbf{b})-\cos^2(\mathbf{m}_0,\mathbf{b})[1+(\alpha_2/\alpha_1)-2\alpha_2\cos(\mathbf{d},\mathbf{b})]\}}{1-\alpha_2\cos^2(\mathbf{d},\mathbf{b})}. \quad (76)$$

Substituting from Eq. 76 into Expression 75 yields the desired sufficient condition for resolution of unequal sources.

Having obtained a necessary condition and a sufficient condition for resolution, it is of interest to examine whether these conditions provide tight bounds on the signal-to-noise ratio required for resolution or these conditions leave a large middle ground where the resolution situation is in question. To examine this issue, we return to the line array geometry of the previous section but this time with R given by Eq. 70. Figure 7 presents the sufficient condition obtained from Eq. 76 when $\sigma_2^2/\sigma_1^2=1000$, so that the strong signal is three orders of magnitude larger than the weak signal.

Also presented for comparison is the necessary condition $\sigma_2^2/\sigma_1^2=1$ which was presented earlier in Fig. 5. Even in this extreme case in which one source is 1000 times stronger than the other, the two curves differ by only about 2 dB over a large range of $M\sigma_1^2/\sigma_0^2$. The necessary condition and the sufficient condition are seen to provide tight bounds on the signal-to-noise ratio required for resolution. Thus, we conclude that two closely spaced sources of unequal strength will be resolved by a $\mathbf{k}_3$-beamformer if the strength of the weaker source is slightly larger than that required for resolution of two sources of equal strength in a similar geometric configuration.

V. CONCLUSION

The inclusion of the signal in the matrix inversion process leads to signal suppression when the maximum possible output signal-to-noise ratio is greater than unity. The effect on output signal-to-noise ratio is particularly dramatic in that strong signals may produce lower output signal-to-noise ratios than weak signals. The effect on the total beamformer output is less dramatic since the decrease in signal response is partially offset by an increase in noise response. Thus, the importance of the signal suppression effect can depend on how the beamformer outputs are to be used. A coherent processor operating on the beamformer output could be seriously affected by the reduced signal-to-noise ratio, while the effects on a direct comparison of beam outputs would be less serious.

With an understanding of this phenomenon, techniques presumably can be developed to overcome the difficulties. Since the effect is not present in the $\mathbf{k}_2$-processor, there seems to be potential payoff in techniques which strive to obtain signal-free estimates of the noise cross-spectral matrix.

The same effect which leads to anomalous suppression of mismatched signals leads to the possibility of resolving closely spaced sources. High output signal to-noise ratios are required in order to achieve resolving power significantly better than the Rayleigh limit. Optimum processing can lead to much better definition of peaks in the scanned output with much deeper valleys between adjacent peaks.

Closely spaced unequal sources can be resolved by a $\mathbf{k}_3$-beamformer if the strength of the weaker source is slightly larger than that required for resolution of two equistrength sources in the same geometric configuration.

The results of this paper are applicable in a variety of situations in which arrays of sensors are used to determine directional properties of propagating waves. These include seismology, radio astronomy, radar, sonar, and measurement of directional properties of ocean waves. In addition, since spectral analysis is essentially the same problem as beamforming with a line array, the results of this paper can easily be reinterpreted and applied to the problem of computing spectrums from correlation functions.

APPENDIX A: DERIVATIONS OF EQS. 21, 22, AND 23

Let

$$\mathbf{R}=\sigma_0^2\mathbf{Q}+\sigma_1^2\mathbf{d}\mathbf{d}^* \quad (A1)$$

so that

$$\mathbf{R}^{-1}=(1/\sigma_0^2)\{\mathbf{Q}^{-1}-\mathbf{Q}^{-1}\mathbf{d}\mathbf{d}^*\mathbf{Q}^{-1}(\sigma_1^2/\sigma_0^2) \times(1+\mathbf{d}^*\mathbf{Q}^{-1}\mathbf{d}\sigma_1^2/\sigma_0^2)^{-1}\}. \quad (A2)$$

Define

$$(S/N)_{max}=\mathbf{d}^*\mathbf{Q}^{-1}\mathbf{d}\sigma_1^2/\sigma_0^2. \quad (A3)$$

To derive Eq. 21, we proceed as follows: From Eqs. A2 and A3,

$$\mathbf{m}^*\mathbf{R}^{-1}\mathbf{m}=(1/\sigma_0^2)\{\mathbf{m}^*\mathbf{Q}^{-1}\mathbf{m}-|\mathbf{m}^*\mathbf{Q}^{-1}\mathbf{d}|^2(\sigma_1^2/\sigma_0^2) \times[1+(S/N)_{max}]^{-1}\}. \quad (A4)$$

Factoring and using Eq. A3 yields

$$\mathbf{m}^*\mathbf{R}^{-1}\mathbf{m}=\frac{\mathbf{m}^*\mathbf{Q}^{-1}\mathbf{m}}{\sigma_0^2} \times\left\{1-\frac{|\mathbf{m}^*\mathbf{Q}^{-1}\mathbf{d}|^2(S/N)_{max}}{(\mathbf{m}^*\mathbf{Q}^{-1}\mathbf{m})(\mathbf{d}^*\mathbf{Q}^{-1}\mathbf{d})[1+(S/N)_{max}]}\right\}. \quad (A5)$$

Using the definition

$$\cos^2(\mathbf{m},\mathbf{d};\mathbf{Q}^{-1}) =|\mathbf{m}^*\mathbf{Q}^{-1}\mathbf{d}|^2/(\mathbf{m}^*\mathbf{Q}^{-1}\mathbf{m})(\mathbf{d}^*\mathbf{Q}^{-1}\mathbf{d}), \quad (A6)$$

Eq. A5 becomes

$$\mathbf{m}^*\mathbf{R}^{-1}\mathbf{m}=\frac{\mathbf{m}^*\mathbf{Q}^{-1}\mathbf{m}}{\sigma_0^2} \times\left\{1-\frac{(S/N)_{max}\cos^2(\mathbf{m},\mathbf{d};\mathbf{Q}^{-1})}{1+(S/N)_{max}}\right\}. \quad (A7)$$

Using the relationship

$$\sin^2(\mathbf{m},\mathbf{d};\mathbf{Q}^{-1})=1-\cos^2(\mathbf{m},\mathbf{d};\mathbf{Q}^{-1}), \quad (A8)$$

$$\mathbf{m}^*\mathbf{R}^{-1}\mathbf{m}=\frac{\mathbf{m}^*\mathbf{Q}^{-1}\mathbf{m}}{\sigma_0^2} \times\left\{\frac{1+(S/N)_{max}\sin^2(\mathbf{m},\mathbf{d};\mathbf{Q}^{-1})}{1+(S/N)_{max}}\right\}. \quad (A9)$$

Equation A7 is the same as Eq. 21, which was to be proven.

To derive Eq. 22, we proceed as follows: From Eqs. A2 and A3,

$$|\mathbf{m}^*\mathbf{R}^{-1}\mathbf{d}|^2=\frac{1}{\sigma_0^4}\left|\mathbf{m}^*\mathbf{Q}^{-1}\mathbf{d}\left(1-\frac{(S/N)_{max}}{1+(S/N)_{max}}\right)\right|^2. \quad (A10)$$

Simplifying,

$$|\mathbf{m}^*\mathbf{R}^{-1}\mathbf{d}|^2=(1/\sigma_0^4)|\mathbf{m}^*\mathbf{Q}^{-1}\mathbf{d}|^2\{1+(S/N)_{max}\}^{-2}. \quad (A11)$$

Using Eq. A6 yields the following result, which is identical with Eq. 22:

$$|\mathbf{m}^*\mathbf{R}^{-1}\mathbf{d}|^2=\frac{(\mathbf{m}^*\mathbf{Q}^{-1}\mathbf{m})(\mathbf{d}^*\mathbf{Q}^{-1}\mathbf{d})\cos^2(\mathbf{m},\mathbf{d};\mathbf{Q}^{-1})}{\sigma_0^4[1+(S/N)_{max}]^2}. \quad (A12)$$

To derive Eq. 23, we proceed as follows: From Eq. A1,

$$\mathbf{Q}=(1/\sigma_0^2)\mathbf{R}-(\sigma_1^2/\sigma_0^2)\mathbf{d}\mathbf{d}^*. \quad (A13)$$

Hence,

$$\mathbf{m}^*\mathbf{R}^{-1}\mathbf{Q}\mathbf{R}^{-1}\mathbf{m}=(1/\sigma_0^2)\mathbf{m}^*\mathbf{R}^{-1}\mathbf{m} -(\sigma_1^2/\sigma_0^2)|\mathbf{m}^*\mathbf{R}^{-1}\mathbf{d}|^2. \quad (A14)$$

Substituting from Eqs. A9 and A12 into Eq. A14 and using Eq. A3 yields

$$\mathbf{m}^*\mathbf{R}^{-1}\mathbf{Q}\mathbf{R}^{-1}\mathbf{m} =\frac{\mathbf{m}^*\mathbf{Q}^{-1}\mathbf{m}}{\sigma_0^4}\left\{\frac{1+(S/N)_{max}\sin^2(\mathbf{m},\mathbf{d};\mathbf{Q}^{-1})}{1+(S/N)_{max}} -\frac{(S/N)_{max}\cos^2(\mathbf{m},\mathbf{d};\mathbf{Q}^{-1})}{\{1+(S/N)_{max}\}^2}\right\}. \quad (A15)$$

Multiplying and dividing the first term in braces in Eq. A15 by $\{1+(S/N)_{max}\}$, and using Eq. A8 yields the following result, which is identical to Eq. 23:

$$\mathbf{m}^*\mathbf{R}^{-1}\mathbf{Q}\mathbf{R}^{-1}\mathbf{m}=\frac{\mathbf{m}^*\mathbf{Q}^{-1}\mathbf{m}}{\sigma_0^4} \times\left\{\frac{1+[2(S/N)_{max}+(S/N)_{max}^2]\sin^2(\mathbf{m},\mathbf{d};\mathbf{Q}^{-1})}{\{1+(S/N)_{max}\}^2}\right\}. \quad (A16)$$

APPENDIX B: DERIVATION OF EQS. 52 AND 72

Let

$$\mathbf{R}=\sigma_0^2\mathbf{I}+\sigma_1^2\mathbf{d}\mathbf{d}^*+\sigma_2^2\mathbf{b}\mathbf{b}^* \quad (B1)$$

and

$$z_d/z_m=(\mathbf{m}^*\mathbf{R}^{-1}\mathbf{m})/(\mathbf{d}^*\mathbf{R}^{-1}\mathbf{d}). \quad (B2)$$

Define

$$\mathbf{V}=\sigma_0^2\mathbf{I}+\sigma_2^2\mathbf{b}\mathbf{b}^*. \quad (B3)$$

Then, letting $\mathbf{V}$ play the role of $\sigma_0^2\mathbf{Q}$ in Eq. A9, Eq. B2 becomes

$$z_d/z_m=\{(\mathbf{m}^*\mathbf{V}^{-1}\mathbf{m})/(\mathbf{d}^*\mathbf{V}^{-1}\mathbf{d})\} \times\{1+\sigma_1^2\mathbf{d}^*\mathbf{V}^{-1}\mathbf{d}\sin^2(\mathbf{m},\mathbf{d};\mathbf{V}^{-1})\}. \quad (B4)$$

By definition,

$$\sin^2(\mathbf{m},\mathbf{d};\mathbf{V}^{-1})=\frac{(\mathbf{m}^*\mathbf{V}^{-1}\mathbf{m})(\mathbf{d}^*\mathbf{V}^{-1}\mathbf{d})-|\mathbf{m}^*\mathbf{V}^{-1}\mathbf{d}|^2}{(\mathbf{m}^*\mathbf{V}^{-1}\mathbf{m})(\mathbf{d}^*\mathbf{V}^{-1}\mathbf{d})}, \quad (B5)$$

so that Eq. B4 may be rewritten as follows:

$$z_d/z_m=\{\mathbf{m}^*\mathbf{V}^{-1}\mathbf{m}+\sigma_1^2[(\mathbf{m}^*\mathbf{V}^{-1}\mathbf{m})(\mathbf{d}^*\mathbf{V}^{-1}\mathbf{d}) -|\mathbf{m}^*\mathbf{V}^{-1}\mathbf{d}|^2]\}/(\mathbf{d}^*\mathbf{V}^{-1}\mathbf{d}). \quad (B6)$$

Let

$$\alpha_2=\frac{(M\sigma_2^2/\sigma_0^2)}{(1+M\sigma_2^2/\sigma_0^2)} \quad (B7)$$

then

$$\mathbf{V}^{-1}=(1/\sigma_0^2)\{\mathbf{I}-\mathbf{b}\mathbf{b}^*\alpha_2/M\}. \quad (B8)$$

Each of the quantities in Eq. B6 will now be examined individually. Recall that $\mathbf{d}$, $\mathbf{b}$, and $\mathbf{m}$ are normalized,

so that

$$\mathbf{m}^*\mathbf{m}=\mathbf{b}^*\mathbf{b}=\mathbf{d}^*\mathbf{d}=M. \quad \text{(B9)}$$

Using Eq. B8,

$$\mathbf{m}^*\mathbf{V}^{-1}\mathbf{m}=(1/\sigma_0^2)[M-|\mathbf{m}^*\mathbf{b}|^2\alpha_2/M] \quad \text{(B10)}$$

or

$$\mathbf{m}^*\mathbf{V}^{-1}\mathbf{m}=(M/\sigma_0^2)[1-\alpha_2\cos^2(\mathbf{m},\mathbf{b})]. \quad \text{(B11)}$$

Similarly,

$$\mathbf{d}^*\mathbf{V}^{-1}\mathbf{d}=(M/\sigma_0^2)[1-\alpha_2\cos^2(\mathbf{d},\mathbf{b})]. \quad \text{(B12)}$$

Again using Eq. B8,

$$|\mathbf{m}^*\mathbf{V}^{-1}\mathbf{d}|^2=(1/\sigma_0^4)|\mathbf{m}^*\mathbf{d}-(\alpha_2/M)\mathbf{m}^*\mathbf{b}\mathbf{b}^*\mathbf{d}|^2$$

or

$$|\mathbf{m}^*\mathbf{V}^{-1}\mathbf{d}|^2=(1/\sigma_0^4)\{|\mathbf{m}^*\mathbf{d}|^2+(\alpha_2/M)^2|\mathbf{m}^*\mathbf{b}|^2|\mathbf{b}^*\mathbf{d}|^2 - (2\alpha_2/M)\,\mathrm{Re}[\mathbf{m}^*\mathbf{b}\mathbf{b}^*\mathbf{d}\mathbf{d}^*\mathbf{m}]\}, \quad \text{(B13)}$$

where Re denotes the real part. Equivalently,

$$|\mathbf{m}^*\mathbf{V}^{-1}\mathbf{d}|^2 =(M/\sigma_0^2)^2\{\cos^2(\mathbf{m},\mathbf{d})+\alpha_2^2\cos^2(\mathbf{m},\mathbf{b})\cos^2(\mathbf{b},\mathbf{d}) - (2\alpha_2/M^3)\,\mathrm{Re}[\mathbf{m}^*\mathbf{b}\mathbf{b}^*\mathbf{d}\mathbf{d}^*\mathbf{m}]\}. \quad \text{(B14)}$$

Substituting from Eqs. B11, B12, and B14 into Eq. B6 and simplifying using Eq. B7 results in the following equation which is identical with Eq. 72:

$$z_d/z_m=\{1+M\sigma_1^2/\sigma_0^2[1-(\alpha_2/\alpha_1)\cos^2(\mathbf{m},\mathbf{b})-\cos^2(\mathbf{m},\mathbf{d}) -\alpha_2\cos^2(\mathbf{d},\mathbf{b})+(2\alpha_2/M^3)\,\mathrm{Re}(\mathbf{m}^*\mathbf{b}\mathbf{b}^*\mathbf{d}\mathbf{d}^*\mathbf{m})]\} \times\{1-\alpha_2\cos^2(\mathbf{d},\mathbf{b})\}^{-1}, \quad \text{(B15)}$$

where

$$\alpha_1=\frac{(M\sigma_1^2/\sigma_0^2)}{(1+M\sigma_1^2/\sigma_0^2)}. \quad \text{(B16)}$$

When $\sigma_1^2=\sigma_2^2$, $\alpha_1=\alpha_2=\alpha$ and Eq. B15 reduces to Eq. 52.

*This work was done while the author was a visiting Research Associate under the sponsorship of the U. S. Navy Professional Development Program and was supported in part by the Office of Naval Research.

[1]F. Bryn, "Optimum Signal Processing of Three-Dimensional Arrays Operating on Gaussian Signals and Noise," J. Acoust. Soc. Am. 34, 289–297 (1962).

[2]W. Vanderkulk, "Optimum Processing of Acoustic Arrays," J. Br. Inst. Radio Eng. 26, 285–292 (1963).

[3]J. P. Burg, "Three-Dimensional Filtering with an Array of Seismometers," Geophysics 29, 693–713 (1964).

[4]H. Mermoz, "Filtrage Adapté et Utilization Optimale d'une Antenne," Proc. NATO Advanced Study Institute on Signal Processing with Emphasis on Underwater Acoustics, Grenoble (1964).

[5]D. Middleton and H. Groginski, "Detection of Random Acoustic Signals by Receiver with Distributed Elements," J. Acoust. Soc. Am. 38, 727 (1965).

[6]P. E. Green, Jr., E. J. Kelly, Jr., and M. J. Levin, "A Comparison of Seismic Array Processing Methods," Geophys. J. R. Astron. Soc. 11, 67–84 (1966).

[7]Y. T. Lo, S. W. Lee, and Q. H. Lee, "Optimization of Directivity and Signal-to-Noise Ratio of an Arbitrary Antenna Array," Proc. IEEE 54, 1033–1045 (1966).

[8]D. J. Edelblute, J. M. Fisk, and G. L. Kinnison, "Criteria for Optimum-Signal-Detection Theory for Arrays," J. Acoust. Soc. Am. 41, 199 (1967).

[9]J. Capon, R. J. Greenfield, and R. J. Kolker, "Multidimensional Maximum-Likelihood Processign of Large Aperture Seismic Array," Proc. IEEE 55 (2) (1967).

[10]H. Cox, "Interrelated Problems in Estimation and Detection I & II," Proc. NATO Advanced Study Institute on Signal Processing with Emphasis on Underwater Acoustics, Enschede, the Netherlands (Aug. 1968).

[11]A. H. Nuttall and D. W. Hyde, "A Unified Approach to Optimum and Suboptimum Processing for Arrays," U. S. Navy Underwater Sound Lab. Rep. No. 992 (Apr. 1969).

[12]J. B. Lewis and P. M. Schultheiss, "Optimum and Conventional Detection Using a Linear Array," J. Acoust. Soc. Am. 49, 1083–1091 (1971).

[13]J. Capon, "High-resolution Frequency-Wavenumber Spectrum Analysis," Proc. IEEE 57, 1408–1418 (1969).

[14]C. D. Seligson, "Comments on High Resolution Frequency-Wave Number Spectrum Analysis," Proc. IEEE 58 (6), 947–949 (1970).

[15]R. N. McDonough, "Degraded Performance of Nonlinear Array Processors in the Presence of Data Modeling Errors," J. Acoust. Soc. Am. 51, 1186–1193 (1972).

[16]H. Cox, "Sensitivity Considerations in Adaptive Beamforming," Proc. NATO Advanced Study Institute on Signal Processing, Loughborough, U.K. (Aug. 1972).

[17]J. Capon and N. R. Goodman, "Probability Distributions of Estimators of Frequency-Wavenumber Spectrum," Proc. IEEE 58 (10), 1785–1786 (1970); correction, Proc. IEEE 59 (1), 112 (1971).

[18]E. Parzen, "Extraction and Detection Problems in Reproducing Kernel Hilbert Spaces," J. SIAM Control 1 (1), 35–62 (1962).

[19]T. Kailath, "RKHS Approach to Detection and Estimation Problems—Part I: Deterministic Signals in Gaussian Noise," IEEE Trans. Inf. Theory IT-17 (5), 530–549 (1971).

[20]M. Born and E. Wolf, *Principles of Optics* (Pergamon, London, 1970), 4th ed.